



TITLE:

Studies on polarographic catalytic hydrogen currents of proteins(Dissertation_全文)

AUTHOR(S):

Kano, Kenji

CITATION:

Kano, Kenji. Studies on polarographic catalytic hydrogen currents of proteins. 京都大学, 1983, 農学博士

ISSUE DATE:

1983-01-24

URL:

<https://doi.org/10.14989/doctor.k2864>

RIGHT:

新 制
農
362

京大附図

STUDIES ON POLAROGRAPHIC CATALYTIC
HYDROGEN CURRENTS OF PROTEINS

KENJI KANO

1982

STUDIES ON POLAROGRAPHIC CATALYTIC
HYDROGEN CURRENTS OF PROTEINS

KENJI KANO

1982

CONTENTS

Introduction	1
Part I. Fundamental Studies on Brdicka Current	4
Chapter 1. Theory of Brdicka Current	4
Theory	4
Summary	8
Chapter 2. Experimental Verification of Theoretical Equation	9
Experimental	9
Results and Discussion	10
Summary	18
Chapter 3. Effects of the Concentration of Buffer Components, pH and Temperature	19
Experimental	19
Results and Discussion	19
Summary	29
Chapter 4. Pulse Polarographic Studies on Brdicka Current	30
Experimental	30
Equations of Brdicka Currrent in Pulse Polarography	31
Results and Discussion	33
Summary	43
Part II. Analytical Applications of Brdicka Current	44
Chapter 5. Trace Analysis of Proteins by Differential Pulse Polarographic Technique	44
Experimental	44
Results and Discussion	45
Summary	48
Chapter 6. Polarographic Study on Enzyme-Inhibitor Interaction	49
Experimental	49
Results and Discussion	51
Summary	69

Chapter 7. Polarographic Study on Interaction between Human IgG and Sheep Antihuman IgG Antiserum and its Analytical	
Application	71
Experimental	71
Results and Discussion	72
Summary	79
Conclusion	81
Acknowledgements	84
References	85

List of Frequently Used Symbols

A:	electrode surface area
C:	concentration in bulk phase
D:	diffusion coefficient
E:	electrode potential
F:	Faraday constant
f_{Co} :	flux of cobalt ion at electrode surface
h:	height of mercury reservoir of dropping mercury electrode
i_{B} :	Brdicka current intensity
K:	dissociation constant
k_{B} :	Brdicka current constant of protein
k_{C} :	intrinsic catalytic activity constant of protein-cobalt complex
k_{d} :	rate constant for decomposition of protein-cobalt complex
k_{f} :	rate constant for formation of protein-cobalt complex
N_{C} :	number of Brdicka-active groups in a protein molecule
N_{S} :	number of cysteine or half-cystine residues in a protein molecule
n_{C} :	number of the total sites, on which protein-cobalt complex can be formed, in a protein molecule
R:	gas constant
T:	absolute temperature
t:	a) time b) Celsius temperature
v:	potential sweep rate
Γ :	surface concentration of protein adsorbed on electrode surface
K:	proportional constant converting protein concentration in bulk phase to Brdicka current intensity
τ :	drop time

INTRODUCTION

Proteins containing sulfhydryl- and/or disulfide-groups possess a marked ability for producing catalytic hydrogen evolution current at mercury electrode.^{1,2)} The characteristic feature of the SS/SH-containing proteins as the hydrogen evolution catalyst is the sharp increase in their catalytic ability upon addition of cobalt salts to the solution. This was first observed by Brdicka³⁾ some fifty years ago, and is usually referred to as polarographic protein wave or Brdicka current after its discoverer. Recently, it has been found that heme proteins, such as cytochromes c containing heme c⁴⁾ and myoglobin containing protoheme,⁵⁾ and S-(ethylsuccinimide)-protein⁶⁾ also produce Brdicka current. These

catalytic currents are observed on d.c. polarogram succeeding the limiting current of cobalt ion, as shown in Fig.1.

Immediately after its discovery, the Brdicka current was applied first to serum protein analysis for diagnosis of cancer and other patients, then to other fields of protein analysis, such as the evaluation of irradiated food

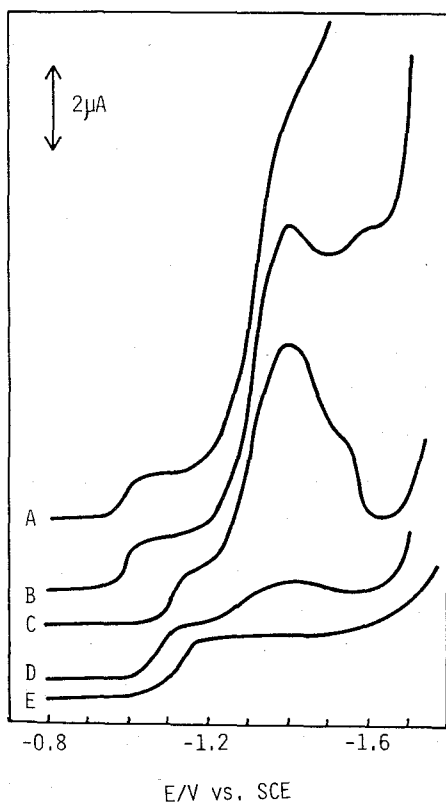


Fig.1 D.c. polarograms of
A) ribonuclease-A, B) bovine serum
albumin, c) cytochrome c,
D) myoglobin, and E) subtilisin
BPN' at $80 \mu\text{g cm}^{-3}$ in ammoniacal
buffer of pH 9.5 containing $2 \times 10^{-4} \text{ mol dm}^{-3} \text{Co}(\text{NH}_3)_6\text{Cl}_3$.

proteins (for reviews, see references^{7,8}). Recently, increased attention has been paid to fundamental aspects of Brdicka current with the intention to develop its analytical applicability (for recent reviews, see references⁹⁻¹³). From the analytical chemistry point of view, the Brdicka current is based on the measurement of the rate (*i.e.* current) of the electrochemical reaction catalyzed by trace amount of proteins present at the mercury electrode surface. Furthermore, the protein are concentrated at the electrode surface by adsorption. Thus, the Brdicka current has a considerably high sensitivity as a tool for protein analysis,¹² together with the comparatively high precision and the usability of the polarographic methods of analysis with the dropping mercury electrode. On the other hand, the Brdicka current is produced only but almost indiscriminately by SS and/or SH containing proteins (and a few other kinds of proteins⁴⁻⁶). This feature of the Brdicka current can be an advantage or disadvantage as analytical demands may be. Also the Brdicka current is sensitive to some extent to the structure of protein and its conformational change.^{4,5,13-16} Accordingly, combination of the high sensitivity of Brdicka current with the selectivity or ability of proteins to recognize other molecules, as seen in enzyme-inhibitor complex formation or antigen-antibody complex formation, may lead to a novel technique of trace analysis of proteins.

In spite of a large number of papers devoted to the study of the fundamentals of Brdicka current, the mechanism of Brdicka current has not fully been understood yet. To advance the analytical application of Brdicka current furthermore, the elucidation of the mechanism is important. Thus the development of the basic theory of Brdicka current which may relate the Brdicka current intensity with various experimental factors in a quantitative way is highly desirable. Recent studies^{12,17-19} have revealed that the Brdicka current is controlled by the rate of supply of cobalt ions to the electrode surface, as well as the surface concentration of proteins adsorbed on electrode surface. Thus, Senda *et al.*²⁰ has proposed a basic equation of the Brdicka current, in which a zero-valent cobalt - protein complex is considered

as an active center to produce Brdicka current.

In this thesis, contribution of the present author to the study on fundamentals and applications of polarographic Brdicka current has been summerized in two parts. Part I deals with fundamental studies on Brdicka current. In chapter 1, the extended theoretical equation of Brdicka current which allows to explain the characteristics of Brdicka current over the wide range of experimental conditions is proposed. Chapter 2 describes experimental verification of the theoretical equation. By this theoretical equation, dependence of Brdicka current on the conditions of electrode system as well as on the concentrations of protein and of cobalt (III) or (II) salt can well be explained. In chapter 3, effects of the concentration of buffer components, pH and temperature on Brdicka current are quantitatively analyzed and the mechanism of Brdicka reaction is discussed. Chapter 4 is concerned with the study on some basic properties of Brdicka current in normal- and differential-pulse polarography. These are reasonably explained by the above theoretical equation. In part II, some applications of Brdicka current to protein analysis are described. Chapter 5 deals with the important features of Brdicka currents obtained with differential pulse polarographic technique. The method allows to detect trace amount of proteins as low as few ng per cm³ under certain conditions. In chapter 6, using d.c.- and differential pulse-polarographic techniques, the complex formation of proteinase (subtilisin BPN') with protein proteinase inhibitors (*Streptomyces* subtilisin inhibitor or plasminostreptin) is studied and the dissociation constants of the (dimeric) enzyme-inhibitor complexes, as low as 10^{-10} mol dm⁻³, are determined. In determining the dissociation constants the multiple equilibrium involving microscopically distinct forms of the complexes has been taken into account. In the final chapter, polarographic study of the interaction between antigen (human IgG) and antibody (sheep antihuman IgG antiserum) is described, and the polarographic immunoassay based on the Brdicka current is discussed.

PART I. FUNDAMENTAL STUDIES ON BRDICKA CURRENT

CHAPTER 1. THEORY OF BRDICKA CURRENT^{a,b)}

Recent studies^{12,17-19)} on fundamentals of Brdicka current have revealed that Brdicka current is controlled by the surface concentration of protein adsorbed on electrode surface and the flux of cobalt ion from the bulk of the solution to electrode surface. Also it is generally accepted^{12,19,21)} that cobalt (III) or (II) ion is reduced to zero valent cobalt, $\text{Co}(0)$, at the potential where Brdicka current is observed and that $\text{Co}(0)$, which is liganded to a Brdicka-active group of protein to form a protein- $\text{Co}(0)$ complex on electrode surface, may catalyze the hydrogen evolution before the complex is decomposed into $\text{Co}(0)$ -amalgam. In this chapter, the author presents an equation of Brdicka current in which the Brdicka current is expressed by a function of the surface concentration of protein adsorbed on electrode surface, the bulk concentration of cobalt ion and two parameters representing the properties of the complex which catalyzes the hydrogen evolution.

THEORY

The mechanism of Brdicka current is not yet fully understood, but it is generally accepted^{12,19,21)} that zero-valent cobalt, $\text{Co}(0)$, which is liganded to a Brdicka-active group of protein to form a protein- $\text{Co}(0)$ complex on electrode surface, may catalyze the hydrogen evolution before the complex is decomposed into $\text{Co}(0)$ -amalgam (see Fig.1-1). The surface concentration (number of moles per cm^2) of the protein- $\text{Co}(0)$ complex is expressed by $n_c \Gamma_0$, where n_c the number of sites on which the protein- $\text{Co}(0)$ complex can be formed in a molecule of protein,

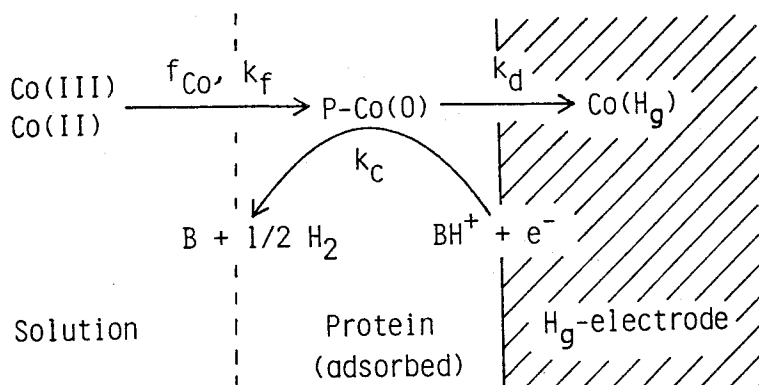


Fig.1-1. The proposed mechanism of Brdicka current.

Γ the surface concentration of protein adsorbed on electrode surface, and θ the fraction of the total available sites occupied by $\text{Co}(0)$ at any instant. Accordingly, the Brdicka current, i_B , may be given by

$$i_B = FAn_c k_c \theta \Gamma \quad (1-1)$$

where F is Faraday constant, A the electrode surface area, and k_c the constant representing the intrinsic activity of the complex to catalyze the hydrogen evolution. If f_{Co} is the flux of cobalt ion at the electrode surface and $(1-\theta)$ is the fraction of the sites which is not occupied, the rate of formation of the complex will be proportional to $f_{\text{Co}} n_c \Gamma (1-\theta)$, and hence is given by $k_f f_{\text{Co}} n_c \Gamma (1-\theta)$, where k_f is the (constant) proportion which forms the complex. The rate of decomposition of the complex into $\text{Co}(0)$ -amalgam may be given by $k_d n_c \Gamma \theta$, where k_d is the constant. At the stationary state we have $k_f f_{\text{Co}} n_c \Gamma (1-\theta) = k_d n_c \Gamma \theta$, or $\theta = (k_f/k_d) f_{\text{Co}} / [1 + (k_f/k_d) f_{\text{Co}}]$. Accordingly, from Eq.(1-1) we get an equation of Brdicka current,

$$i_B = FAn_c k_c \Gamma \frac{(k_f/k_d) f_{\text{Co}}}{1 + (k_f/k_d) f_{\text{Co}}} \quad (1-2)$$

In this derivation, it is assumed that all the protein- $\text{Co}(0)$ complexes

in a protein molecule are identical in their catalytic activity of hydrogen evolution as well as in their kinetics of formation and decomposition. If they are not identical, Eq.(1-2) should be replaced by an exact equation,

$$i_B = F A f_{Co} \Gamma \sum_i \frac{k_c^i (k_f^i/k_d^i)}{1 + (k_f^i/k_d^i) f_{Co}} \quad (1-3)$$

where k_c^i , k_f^i and k_d^i ($i = 1, 2, \dots, n_c$) are the constants for the i -th complex. This consideration indicates that in Eq.(1-2) the constants k_c , k_f and k_d should be interpreted as the average constants of all the complexes.

At extremely low concentration of cobalt ion $(k_f/k_d) f_{Co} \ll 1$ (or $H_2 \gg C_{Co}$, see Eq.(1-7)), so that we have

$$i_{B, C_{Co} \rightarrow 0} = F A k_B f_{Co} \Gamma \quad (1-4)$$

with

$$k_B = n_c k_c (k_f/k_d) = \sum_i k_c^i (k_f^i/k_d^i) \quad (1-5)$$

At the dropping mercury electrode, f_{Co} is given by Ilkovic equation,

$$f_{Co} = (7 D_{Co} / 3 \pi t)^{1/2} C_{Co} \quad (1-6)$$

where t is the time, D_{Co} and C_{Co} are the diffusion coefficient and concentration of cobalt ion, respectively. On substituting Eq.(1-6) into Eq.(1-2), we get

$$i_B = H_1 C_{Co} / (H_2 + C_{Co}) \quad (1-7)$$

with

$$H_1 = F A n_c k_c \Gamma \quad (1-8)$$

and

$$H_2 = (k_d/k_f) (3\pi t/7D_{Co})^{1/2} \quad (1-9)$$

The surface area of the dropping mercury electrode is given by $A = 0.0085m^{2/3} t^{2/3} = A_0 t^{2/3}$, A_0 being a constant at a constant mercury flow rate. Exact mathematical expression to predict Γ for a given system is very complicated, except Koryta's treatment²²⁾ of the limiting case of extremely strong adsorption of protein. If Koryta's treatment is valid, at low concentration of protein we have

$$\Gamma = (12D_p t/7\pi)^{1/2} C_p \quad (1-10)$$

where D_p and C_p are the diffusion coefficient and concentration of protein. Thus we have at low concentration of protein

$$H_1 = F A_0 n_c k_c (12D_p/7\pi)^{1/2} t^{7/6} C_p \quad (1-11)$$

then at extremely low concentration of cobalt ion ($C_{Co} \ll H_2$)

$$i_{B, C_p \rightarrow 0, C_{Co} \rightarrow 0} = F A_0 n_c k_c (k_f/k_d) (2/\pi) (D_p D_{Co})^{1/2} t^{2/3} C_p C_{Co} \quad (1-12)$$

and at extremely high concentration of cobalt ion ($C_{Co} \gg H_2$)

$$i_{B, C_p \rightarrow 0, C_{Co} \rightarrow \infty} = F A_0 n_c k_c (12D_p/7\pi)^{1/2} t^{7/6} C_p \quad (1-13)$$

At high concentration of protein, the surface of dropping mercury electrode may be considered as saturated with adsorbed protein for the whole life of a mercury drop, that is, $\Gamma = \Gamma^{\max}$. Hence we have

$$H_1 = F A_0 n_c k_c \Gamma^{\max} t^{2/3} \quad (1-14)$$

then, at extremely low concentration of cobalt ion ($C_{Co} \ll H_2$)

$$i_{B, \Gamma=\Gamma^{\max}, C_{Co} \rightarrow 0} = FA_0 n_c k_c (k_f/k_d)^{\max} (7D_{Co}/3\pi)^{1/2} t^{1/6} C_{Co} \quad (1-15)$$

and at extremely high concentration of cobalt ion ($C_{Co} \gg H_2$)

$$i_{B, \Gamma=\Gamma^{\max}, C_{Co} \rightarrow \infty} = FA_0 n_c k_c \Gamma^{\max} t^{2/3} \quad (1-16)$$

SUMMARY

Basic equation of Brdicka current is presented, in which Brdicka current is expressed by a function of the surface concentration of protein, the bulk concentration of cobalt ion and two parameters, $n_c k_c$ and k_f/k_d , where n_c is the number of the total sites, on which the complex can be formed, in a protein molecule, and k_c and k_f/k_d are the (average) constants representing the intrinsic catalytic activity and the life time, respectively, of the complex.

CHAPTER 2. EXPERIMENTAL VERIFICATION OF THEORETICAL EQUATION^{b, c)}

In this chapter, dependence of Brdicka current on the conditions of electrode system as well as on the concentrations of protein and of cobalt (III) or (II) salt has experimentally been investigated to verify the prediction of the theoretical equation derived in the preceding chapter. Method to determine the two parameters $n k_c$ and k_f/k_d , representing the properties of the complex to catalyze the hydrogen evolution, is proposed.

EXPERIMENTAL

Materials:

Bovine pancreas ribonuclease-A (RNase, Type I-A, lot No. 58C-0116) and horse heart cytochrome c (Cyt-c, Type VI, lot No. 78C-7040) were products of Sigma Chemical Co. and used without further purification. S-(ethylsuccinimide)-ribonuclease-A (NEM-RNase) was prepared according to Smith *et al.*²³⁾. The concentrations of proteins were checked spectrophotometrically.^{24,25)} Other chemicals used were of reagent grade quality. Triply distilled water was used to prepare the electrolysis solution.

Apparatus:

Polarograms and current-time curves were recorded with a Fuso potentiostat 311, equipped with a Yokogawa X-Y recorder 3077. All measurements were made under potentiostatic conditions with a three-electrode system consisting of a dropping mercury working electrode (dme), a platinum wire auxiliary electrode, and a saturated calomel reference electrode (SCE). The characteristics of the dme were $m = 0.687 \text{ mg s}^{-1}$ and $\tau = 9.80 \text{ s}$ at $h = 21.0 \text{ cm Hg}$ and $E = -1.40 \text{ V vs. SCE}$ in an ammoniacal

buffer.

Electrochemical Measurements:

All measurements were made in an H-type cell immersed in a thermostat controlled at 25.0 ± 0.5 °C. Buffer solution containing $0.1 \text{ mol dm}^{-3} \text{ NH}_3$, $0.1 \text{ mol dm}^{-3} \text{ NH}_4\text{Cl}$ and $0.1 \text{ mol dm}^{-3} \text{ KCl}$ (pH 9.5, ionic strength 0.2 mol dm^{-3}) was used as the base solution. Ten ml of the base solution was transferred into the polarographic cell and deaerated for 15 to 20 min by passing nitrogen gas, which had previously been passed through a solution of the same composition as the buffer solution. Then, aliquot of solutions of proteins and $\text{Co}(\text{NH}_3)_6\text{Cl}_6$ were introduced into the deaerated base solution with a microsyringe under nitrogen atmosphere. In the current measurement, instantaneous currents were taken and the catalytic currents were measured from the cobalt limiting currents.

RESULTS AND DISCUSSION

Experimental Verification of Theory:

Fig.2-1 shows polarograms of RNase in the base solution containing different concentration of hexaaminecobalt (III) chloride, $\text{Co}(\text{III})$. In the following we shall discuss the Brdicka current at -1.4 V , where most proteins are so strongly adsorbed on mercury electrode surface that Γ can be calculated by Koryta equation.^{20,22,26)}

Fig.2-2 shows the parabolic dependence of Brdicka current, i_B , on the concentration of $\text{Co}(\text{III})$, $C_{\text{Co}(\text{III})}$. Fig.2-3, in which $1/i_B$ is plotted against $1/C_{\text{Co}(\text{III})}$, most clearly demonstrated that the dependence of i_B on $C_{\text{Co}(\text{III})}$ is well reproduced by Eq.(1-7), that is, $1/i_B = 1/H_1 + (H_2/H_1)(1/C_{\text{Co}})$. This had empirically been demonstrated by Klumpar²⁷⁾ as early as in 1940 s. Fig.2-4 shows the dependence of i_B on C_p ; i_B first increases linearly with increasing C_p (Eqs.(1-11) to (1-13)), but approaches a saturation value at high C_p (Eqs.(1-14) to

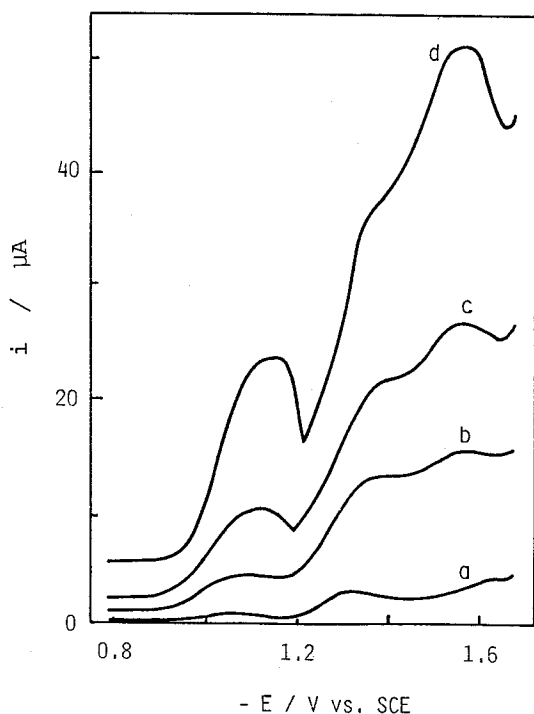
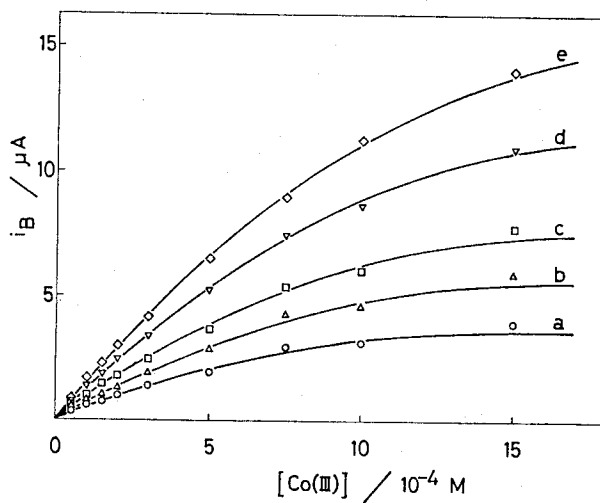


Fig.2-1. D.c. polarograms of $4 \mu\text{g cm}^{-3}$ RNase in the base solution containing Co(III) of a) 1, b) 5, c) 10, and d) $20 \times 10^{-4} \text{ mol dm}^{-3}$.

Fig.2-2. Variation of the Brdicka current of $4 \mu\text{g cm}^{-3}$ RNase with the concentration of Co(III) at the dme: $t =$ a) 2, b) 3, c) 4, d) 6 and e) 8 s.



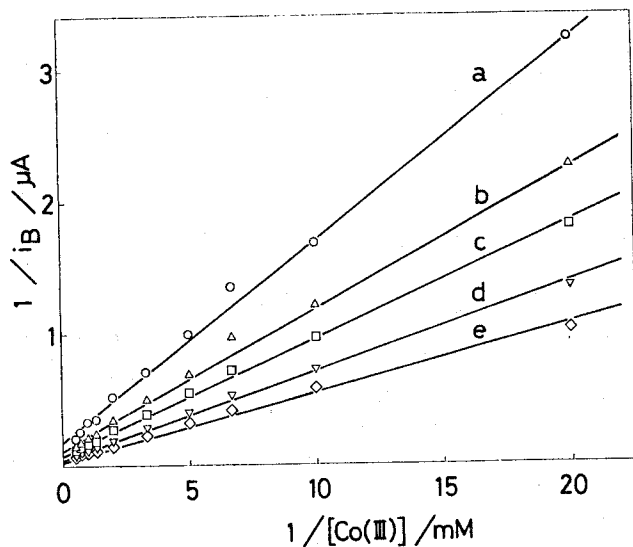


Fig.2-3. Plots of the reciprocal of the Brdicka current against the reciprocal of Co(III) concentration for the Brdicka current of RNase at $t =$ a) 2, b) 3, c) 4, d) 6, and e) 8 s. The data are the same as those in Fig.2-2.

(2-16)).

The parameters H_1 and H_2 were determined by fitting the i_B vs. $C_{Co(III)}$ curves to Eq.(1-7) with the aid of a Facom M-200 Computer in Data Processing Center of Kyoto University for $C_p = 4 \mu g cm^{-3}$ and $t = 2$ to 8 s, where Γ can be evaluated by Koryta equation (Fig.2-5), and for

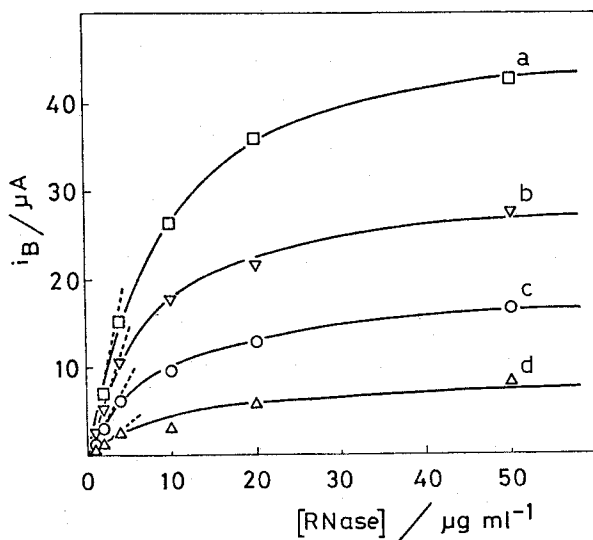


Fig.2-4. Variation of the Brdicka current with the concentration of RNase in the base solution containing a) 2, b) 5, c) 10, and d) $20 \times 10^{-4} mol dm^{-3}$ of Co(III).

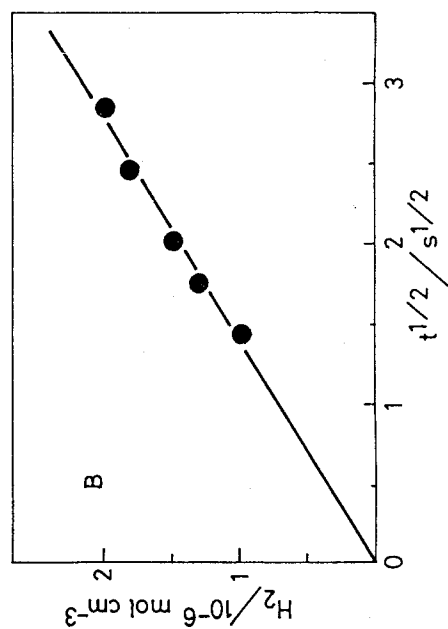
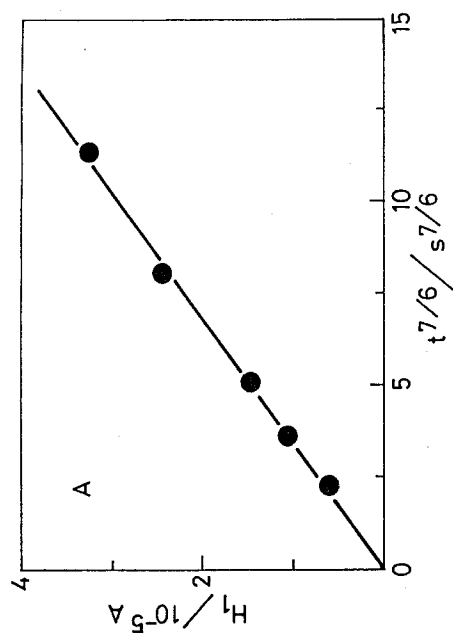


Fig.2-5. Time dependence of A) H_1 and B) H_2 parameters for the Brdicka current of $4 \mu\text{g cm}^{-3}$ RNase.

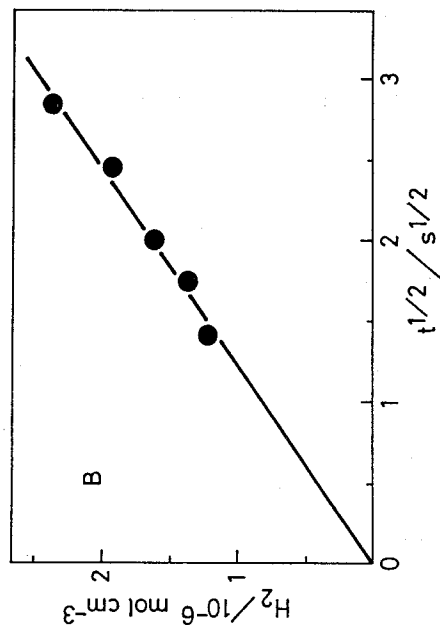
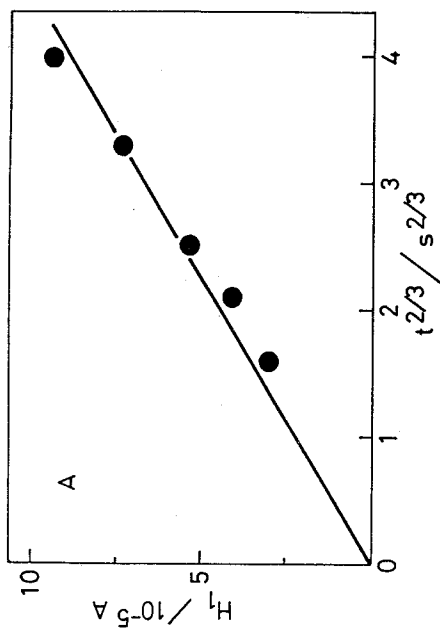


Fig.2-6. Time dependence of A) H_1 and B) H_2 parameters for the Brdicka current of $50 \mu\text{g cm}^{-3}$ RNase.

$C_p = 50 \mu\text{g cm}^{-3}$ and $t = 2$ to 8 s, where $\Gamma = \Gamma^{\text{max}}$ (Fig.2-6). Regression analysis was performed by means of SALS program (copyright: SALS group²⁸). As seen on Figs.2-5 and 2-6 the H_2 parameters depend linearly on $t^{1/2}$ for both $C_p = 4$ and $50 \mu\text{g cm}^{-3}$, whereas the H_1 parameters depend linearly on $t^{7/6}$ or $t^{2/3}$ at $C_p = 4$ or $50 \mu\text{g cm}^{-3}$, respectively. The results agree well with the prediction of Eqs.(1-9), (1-11) and (1-14). Similarly, good agreement between theory and experimental results for the dependence of H_1 and H_2 parameters on the time was obtained also with the Brdicka current of Cyt-c.

According to Eq.(1-8), H_1 should vary with C_p , since Γ depends on C_p for a given system. Fig.2-7 shows the dependence of H_1 on C_p for the Brdicka current of RNase. At relatively low C_p H_1 increases linearly with C_p , and the slope of the linear part of H_1 vs. C_p plots is well explained by Koryta equation or Eq.(1-11) (see Fig.2-5A), giving the $n_c k_c$ value of the protein if its D_p is known. On the other hand, H_2 depends linearly on $t^{1/2}$ in the concentration range between $C_p = 4$ and $50 \mu\text{g cm}^{-3}$ (see Figs.2-5B and 2-6B), giving the k_f/k_d value of the protein by Eq.(1-9) if D_{Co} is known. At extremely low concentration of protein ($C_p = 1 \mu\text{g cm}^{-3}$), however, the linearity of H_2 vs. $t^{1/2}$ plots was not extremely valid. This apparent disagreement between theory and experimental results is likely to be explained by an advanced theory based on more elaborated reaction mechanism,^{c)} but we shall not go here

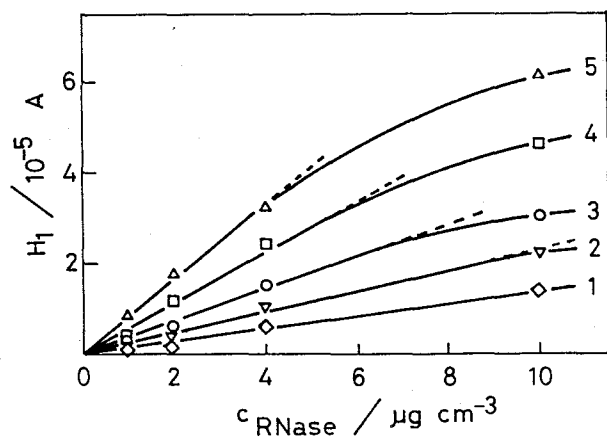


Fig.2-7. Dependence of H_1 parameter on the concentration of RNase for the Brdicka current of RNase at dme; $t = 1) 2, 2) 3, 3) 4, 4) 6, \text{ and } 5) 8$ s.

into the details.

Many author had reported the drop time dependence of the Brdicka current or the value of the exponent x in the expression of $i_B = (\text{const.})t^x$. When C_{Co} is extremely small, x is $2/3$ (kinetic control characteristic) at small C_p and becomes to be $1/6$ (diffusion control characteristic) with increase in C_p .^{16,19,29} These reported values are well explained by Eqs.(1-12) and (1-15).^{16,20} On the other hand, when C_{Co} is large, x varies from $7/6$ to $2/3$ with increase in C_p .^{30,31} If $H_2 \ll C_{Co}$, Eq.(1-7) can be reduced to $i_B = H_1$, which predicts $x = 7/6$ (surface kinetic control characteristic²⁾) at small C_p (Eqs.(1-11) and (1-13)) and $x = 2/3$ (kinetic control characteristic) at large C_p (Eqs.(1-14) and (1-16)). Accordingly, Eq.(1-2) can also predict the general dependence of the Brdicka current on the drop time.

Brdicka Current Constants of Brdicka Active Groups:

Table 2-1 shows the $n_c k_c$ and k_f/k_d values at -1.40 V of three proteins having different kinds of Brdicka-active groups in 0.1 mol dm^{-3} NH_3 , 0.1 mol dm^{-3} NH_4Cl , and 0.1 mol dm^{-3} KCl (pH 9.5) at $25^\circ C$. Preliminary experiment showed that the $n_c k_c/N_c$ and k_f/k_d values of other SH- and/or SS-containing proteins were nearly equal to those of RNase. Myoglobin, which contains protoheme group, is Brdicka active,⁵⁾ but its catalytic activity ($k_B = 0.22 \times 10^{12} \text{ cm}^2 \text{ mol}^{-1}$) is small and hence could not be evaluated by the present method. Other -SR groups, such as $-SCH_3$,³⁾ $-SC_2H_5$,³²⁾ $-SCH_2COOH$,³³⁾ $-SCH_2CONH_2$,⁶⁾ $-SCH_2C_6H_5$,³⁴⁾ and $-SO_3H$ ³³⁾ are known to be Brdicka-inactive. In this table the $n_c k_c/N_c$ values of the three proteins containing different Brdicka-active groups are nearly constant. This fact indicates that the difference in the Brdicka current activity as expressed by k_B/N_c of the Brdicka-active groups should first be attributed to the difference in the stability (or life time) of the complexes. This result also indicated that the Brdicka-active groups may play the most important role as a ligand to form the complex, though other groups such as amino, carboxyl, and peptide groups also may function as ligands to form the complex.

Table 2-1. Brdicka Current Constants of Proteins with Cobalt(III) or (II) at E = -1.4 V in 0.1 mol dm⁻³ NH₃, 0.1 mol dm⁻³ NH₄Cl and 0.1 mol dm⁻³ KCl (pH 9.5) at 25 °C.

Protein	Cobalt	Active Group	N _c ^{a)}	$\frac{n k}{c c} \frac{1}{10^4 s^{-1}}$	$\frac{n k}{c c} \frac{1}{10^3 s^{-1}}$	$\frac{k_f}{k_d} \frac{1}{10^8 cm^2 smol^{-1}}$	$\frac{k}{N_c} \frac{1}{10^{12} cm^2 mol^{-1}}$
RNase	Co(III)	-SH	8	2.1	2.6	4.6	1.2
NEM-RNase	Co(III)	$\begin{array}{c} -SCH-CO-NC_2H_5 \\ \\ CH_2-CO^+ \end{array}$	8	1.8	2.3	2.4	0.55
Cyt-c	Co(III)	Heme-c ^{b)}	1	0.28	2.8	13.0	3.6
RNase	Co(II)	-SH	8	0.61	0.76	9.1	0.69

a) Number of Brdicka-active groups in a protein molecule.

b) The 6th ligand is methionine.

Brdicka Current Constants of Co(III) and Co(II):

Brdicka current was also observed in the presence of cobalt (II) chloride, Co(II), instead of Co(III), but the Brdicka current of Co(II) was less than that of Co(III). Table 2-1 also shows the $n_c k_c$ and k_f/k_d values of RNase with Co(II). The small Brdicka current or small k_B values of Co(II) was revealed to result from small $n_c k_c$ value. The difference between the $n_c k_c$ values of Co(II) and Co(III) must be attributed to the difference in the ligand-substitution lability of cobalt complex ion, that is, Co(II) is substitution labile and Co(III) is substitution inert.³⁵⁾ Above result indicates that the intrinsic activity and the stability of the protein-Co(0) complex are also influenced by the ligands of cobalt complex ion in solution, and that different kinds of protein-Co(0) complexes, different ligand complexes, are generated on electrode surface from Co(III) and Co(II).

Effect of Electrode Potential:

Fig.2-8 shows the dependence of the $n_c k_c$ and k_f/k_d of RNase on the electrode potential, E , Γ being estimated by Koryta equation. Plot A in Fig.2-8 indicates that the $n_c k_c$ can be expressed by $n_c k_c = (\text{const.}) \exp(-\alpha n F E) / RT$ with $\alpha n = 0.3$. Also, plot B in Fig.2-8 shows that the k_f/k_d value of RNase changes with the electrode potential and decreases with increasing negative potential. The dependence of k_f/k_d on E should in part be due to the conformational change of protein

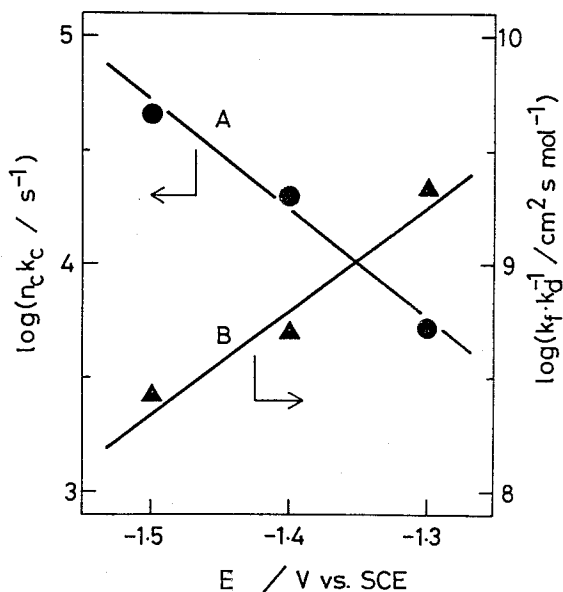


Fig.2-8. Dependence of A) $n_c k_c$ and B) k_f/k_d on the electrode potential for the Brdicka current of $4 \mu\text{g cm}^{-3}$ RNase.

adsorbed on electrode surface.

In conclusion we can state that the Brdicka current is well described by Eqs.(1-2) to (1-16), in which the current is expressed as a function of the surface concentration (or bulk concentration) of protein and the bulk concentration of cobalt ion with two parameters, $n_c k_c$ and k_f/k_d , or three constants, that is, n_c the number of the total sites (or Brdicka-active groups), on which a protein-Co(0) complex can be formed, in a protein molecule; k_c the (average) constant representing the intrinsic activity of the complex to catalyze the hydrogen evolution; and k_f/k_d the (average) constant representing the stability or the life time of the complex.

SUMMARY

The theoretical equation derived in chapter 1 has been experimentally verified on the dependence of Brdicka current on the conditions of electrode system as well as on the concentrations of protein and cobalt (III) or (II) salt. The method to determine the two parameters $n_c k_c$ and k_f/k_d , representing the properties of the complex to catalyze the hydrogen evolution, has been established.

Brdicka current activities $k_B = n_c k_c (k_f/k_d)$ or $n_c k_c$ and k_f/k_d of SS (or SH) group, heme-c group and S-(ethylsuccinimide) group were determined. The difference in their activity between these three groups has been found mainly due to the difference in the stability.

CHAPTER 3. EFFECTS OF THE CONCENTRATION OF BUFFER COMPONENTS, pH AND TEMPERATURE^{d,e)}

Effects of various experimental factors, such as the concentration of buffer components, ionic strength, pH, and temperature, on Brdicka current have been studied by many workers (for review, see references^{2,36,37)}), but their analysis and interpretation have been limited to qualitative ones. This is probably due to the lack of theoretical equation of Brdicka current. In this chapter, the effects of the concentration of buffer components, pH and temperature on Brdicka current have quantitatively been investigated on the basis of the theoretical equation of Brdicka current derived in chapter 1, and the mechanism of the Brdicka reaction has been discussed in some details.

EXPERIMENTAL

As the base solutions, 0.05 to 0.3 mol dm⁻³ NH₃-NH₄Cl buffers of pH 7.91 to 10.32 were used. The ionic strength of the base solution was adjusted to 0.2 mol dm⁻³ with KCl. For recording the current, the drop time was regulated at $\tau = 4.08$ s, with a Yanagimoto drop controller P-8-RT. Temperature was controlled thermostatically at 10.0 to 40.0 °C. Other details of experimental procedures were described in chapter 2.

RESULTS AND DISCUSSION

Effect of Buffer Concentration:

Fig.3-1 shows the dependence of the Brdicka wave of RNase (4 µg cm⁻³) at three different concentration of ammoniacal buffer, $C_{\text{amm}} = [\text{NH}_3] +$

$[\text{NH}_4^+] = 0.1, 0.2 \text{ and } 0.3 \text{ mol dm}^{-3}$ and at $\text{pH} = 9.5$ and $I = 0.2 \text{ mol dm}^{-3}$. The height of the first wave increases with increasing C_{amm} as reported by many workers.³⁷⁻³⁹⁾ The values of k_B at -1.4 V obtained according to Eq.(1-4) are plotted against C_{amm} as shown in Fig.3-2. The k_B value increases with C_{amm} , which agrees with the results of Cyt-c obtained by Ikeda *et al.*³⁹⁾ In order to strictly investigate the effect of

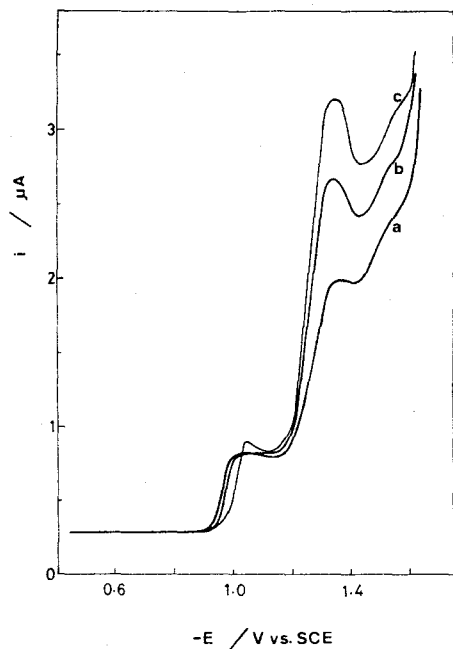


Fig.3-1. D.c. polarograms of $4 \mu\text{g cm}^{-3}$ RNase in the presence of $2 \times 10^{-4} \text{ mol dm}^{-3}$ Co(III) in ammoniacal buffer at $\text{pH } 9.5$ and $C_{\text{amm}} = \text{a) } 0.1, \text{ b) } 0.2$ and $\text{c) } 0.3 \text{ mol dm}^{-3}$.

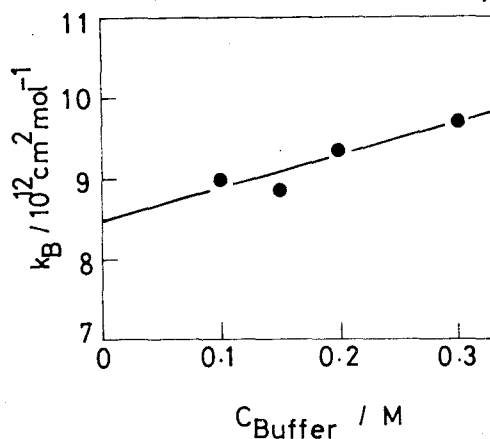


Fig.3-2. Dependence of k_B on the ammoniacal buffer concentration. The k_B values were estimated at $C_P = 4 \mu\text{g cm}^{-3}$, $\text{pH } 9.5$, $E = -1.4 \text{ V}$ and 25°C .

the concentration of C_{amm} on the Brdicka current, the values of $n_c k_c$ and k_f/k_d at various C_{amm} were obtained by analyzing the dependence of the Brdicka current on $C_{\text{Co(III)}}$, according to Eqs.(1-7) to (1-11), and plotted against C_{amm} (Fig.3-3). The $n_c k_c$ value, referring to the intrinsic activity of protein-Co(0) complex, increases linearly with C_{amm} from 0.1 to 0.3 mol dm^{-3} . Whereas the k_f/k_d value, referring to the stability of the complex, somewhat decreases with C_{amm} .

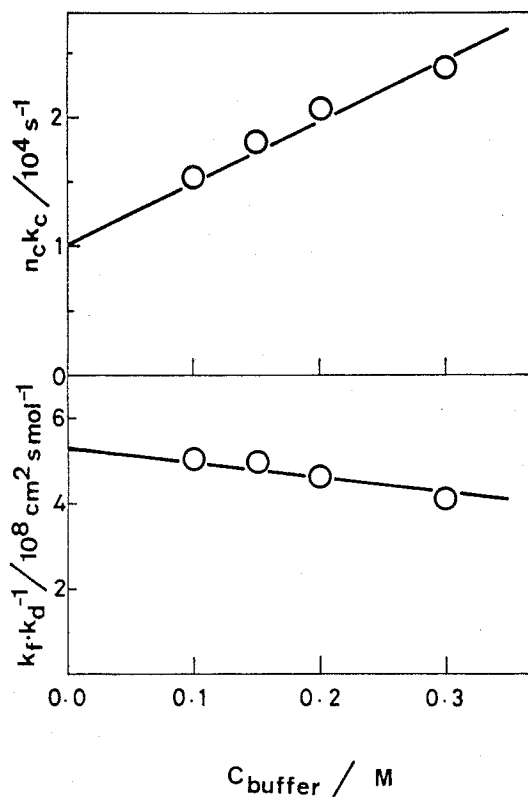


Fig.3-3. Dependence of $n_c k_c$ and k_f/k_d on the ammoniacal buffer concentration.

These values were estimated at $C_p = 4 \mu\text{g cm}^{-3}$, pH 9.5, $E = -1.4 \text{ V}$ and 25°C .

The increase in $n_c k_c$ with C_{amm} could be interpreted as the increase in acidic component of buffer salt, *i.e.* ammonium ion, which works as a proton doner in the Brdicka reaction. This interpretation agrees well with those of many workers (see references^{2,36,37}). Moreover, the extrapolated $n_c k_c$ value in $n_c k_c$ vs. C_{amm} plot to the intercept, $(n_c k_c)_0$, should correspond to the catalytic activity of protein-Co(0) complex in the Brdicka reaction where a proton doner is water molecule, according to Ikeda *et al.*³⁹) Then, on assuming that n_c value is independent of C_{amm} , the present results on the effect of C_{amm} on $n_c k_c$ can be expressed by the following empirical formula,

$$k_c = k_c^{\text{H}_2\text{O}} + k_c^{\text{NH}_4^+} [\text{NH}_4^+] \quad (3-1)$$

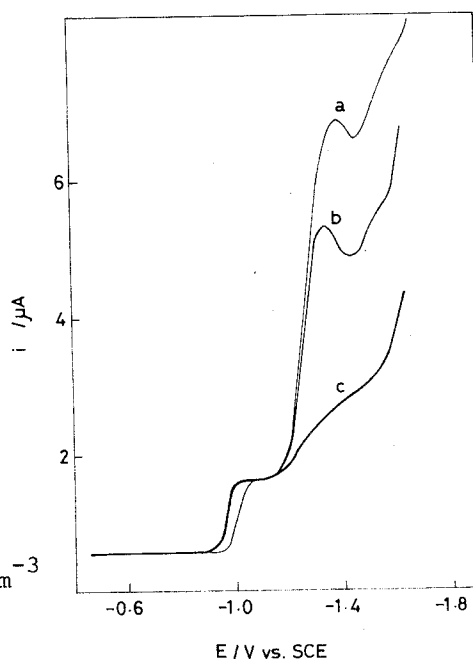
where, $k_c^{H_2O}$ is the constant representing the intrinsic catalytic activity of protein-Co(0) complex in the catalytic reaction where water molecule plays as a proton donor, and $k_c^{NH_4^+}$ the proportional constant representing the intrinsic catalytic activity of the complex in the reaction where ammonium ion plays as a proton donor.

The slight decrease in k_f/k_d value with C_{amm} suggests that an ammonia molecule, which is a ligand of cobalt complex ion in solution, stabilizes the cobalt amine complex³⁸⁾ and participates competitively in the complex formation between protein and Co(0). This is supported by observation that the reduction step of Co(II) to Co(0) shifts negatively with increase in C_{amm} (Fig.3-1). An advanced theory based on more elaborated reaction mechanism^{e,40)} was proposed, but we shall not go here into the details. The extrapolated k_f/k_d value in the k_f/k_d vs. C_{amm} plot to the intercept, $(k_f/k_d)_0$, should represent the stability of protein-Co(0) complex at $[NH_3] = 0$, although the effect of ammonia molecules coordinated to cobalt complex ion in bulk solution is involved.

Effect of pH:

Fig.3-4 shows d.c. polarograms of the protein wave of $4 \mu g \text{ cm}^{-3}$ RNase in 0.2 mol dm^{-3} ammoniacal buffer containing $2 \times 10^{-4} \text{ mol dm}^{-3}$ Co(III) at pH 8.4, 9.5 and 10.3. The catalytic current increases to a great extent with increasing pH. The reduction step of Co(II) to Co(0) shifts to more negative potential with increase in pH, which is interpreted

Fig.3-4. D.c. polarograms of $4 \mu g \text{ cm}^{-3}$ RNase in the presence of $2 \times 10^{-4} \text{ mol dm}^{-3}$ Co(III) in ammoniacal buffer at pH = a) 10.3, b) 9.5, and c) 8.4.



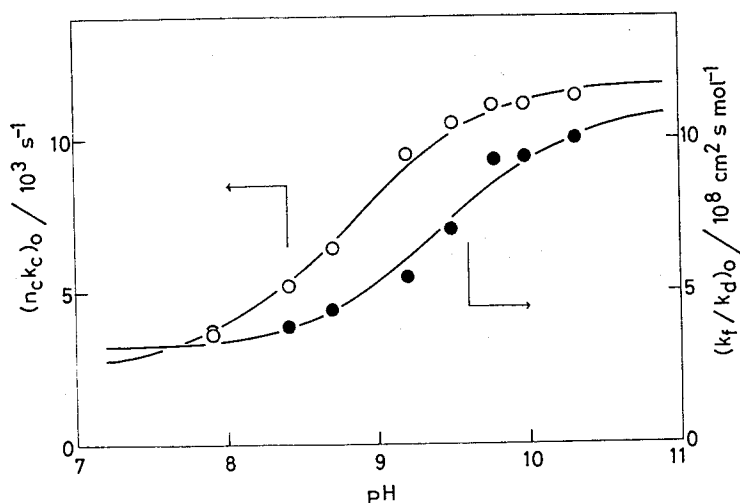


Fig.3-5. Plots of $(n_c k_c)_0$ and $(k_f/k_d)_0$ against pH; data obtained in ammoniacal buffer containing $4 \mu\text{g cm}^{-3}$ RNase at -1.4 V and 25°C . Solid lines are regression curves (see text).

as due to the increase in the concentration of ammonia molecule, which may stabilize cobalt complex ion in solution, as described in previous section. The observed pH-dependence of Brdicka current involves evidently a complicated origin, since the above experimental procedure alters the concentrations of the buffer components as well as pH. In order to eliminate the effect of buffer components,³⁹⁾ $n_c k_c$ and k_f/k_d vs. C_{amm} plots were extrapolated to $C_{\text{amm}} = 0$, and the extrapolated values $(n_c k_c)_0$ and $(k_f/k_d)_0$ were obtained at various pH from 7.9 to 10.3. Fig.3-5 shows the results: the $(n_c k_c)_0$ and $(k_f/k_d)_0$ value increased sigmoidally with pH, but $(n_c k_c)_0$ began to increase at lower pH than in the case of $(k_f/k_d)_0$.

We assume that the pH effect of $(n_c k_c)_0$ and $(k_f/k_d)_0$ was attributed to the ionization of the functional group in RNase (probably electrochemically reduced SH group, see below), which participates in the complex formation between protein and cobalt, and proposed a scheme as shown in Fig.3-6. Two forms of ionization state of the functional group in protein, protonated and non-protonated, participate in the Brdicka reaction^{38,41)} with different values of k_f , k_d and k_c , and the equilibrium

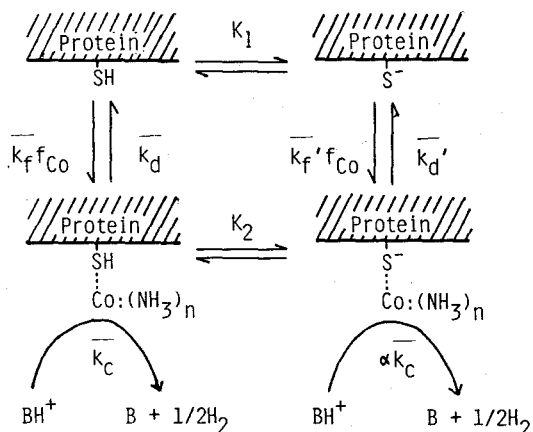


Fig.3-6. Hypothetical scheme of the Brdicka reaction involving ionization of functional group, referred to -SH, in adsorbed protein.

of the protonic dissociation of the functional group is affected by the interaction of the functional group with cobalt.

Here the surface concentration of protein-SH, protein-S⁻, protein-SH-Co(0) complex, and protein-S⁻-Co(0) complex in Fig.3-6 are expressed by $n_c \Gamma \Theta_u$, $n_c \Gamma \Theta_v$, $n_c \Gamma \Theta_w$, and $n_c \Gamma \Theta_x$. Then we have

$$\Theta_u + \Theta_v + \Theta_w + \Theta_x = 1 \quad (3-2)$$

and

$$K_1 = \frac{[n_c \Gamma \Theta_v] [H^+]}{[n_c \Gamma \Theta_u]} \quad (3-3)$$

$$K_2 = \frac{[n_c \Gamma \Theta_x] [H^+]}{[n_c \Gamma \Theta_w]} \quad (3-4)$$

At stationary state, we have

$$n_c \Gamma \Theta_u \bar{k}_f \bar{f}_{Co} = n_c \Gamma \Theta_w \bar{k}_d \quad (3-5)$$

where \bar{k}_f and \bar{k}_d are the pH-independent proportions which forms and

decomposes the complex at $C_{amm} = 0$. From the Eqs.(3-2) to (3-5), we can get

$$n_c \Gamma_w^\theta = n_c \Gamma \frac{\overline{k_f} [H^+] f_{Co}}{\overline{k_d} [H^+] + \overline{k_d} K_1 + f_{Co} \overline{k_f} ([H^+] + K_2)} \quad (3-6)$$

$$n_c \Gamma_x^\theta = n_c \Gamma \frac{\overline{k_f} K_2 f_{Co}}{\overline{k_d} [H^+] + \overline{k_d} K_1 + f_{Co} \overline{k_f} ([H^+] + K_2)} \quad (3-7)$$

Assuming that the intrinsic catalytic activity of protein-S⁻-Co(0) complex is α times of that of protein-SH-Co(0) complex, the Brdicka current at $C_{amm} = 0$ can be expressed by

$$i_{B, C_{amm} \rightarrow 0} = FA(n_c \overline{k_c}) \Gamma(\theta_w + \alpha \theta_x) \quad (3-8)$$

where $\overline{k_c}$ is the constant representing the intrinsic catalytic activity of the complex at $C_{amm} = 0$. Upon substituting Eqs.(3-6) and (3-7) into Eq.(3-8), we can get

$$i_{B, C_{amm} \rightarrow 0} = FA(n_c \overline{k_c})_0 \Gamma(k_f/k_d)_0 f_{Co} \frac{1}{1 + (k_f/k_d)_0 f_{Co}} \quad (3-9)$$

where

$$(n_c \overline{k_c})_0 = (n_c \overline{k_c}) \frac{K_2 + [H^+]}{[H^+] + K_2} \quad (3-10)$$

$$(k_f/k_d)_0 = (\overline{k_f}/\overline{k_d}) \frac{K_2 + [H^+]}{K_1 + [H^+]} \quad (3-11)$$

The values of K_1 , K_2 and α were determined by fitting the $(n_c \overline{k_c})_0$ and $(k_f/k_d)_0$ vs. pH plots to the curves represented by Eqs.(3-10) and (3-11), respectively. The results were $pK_1 = 9.48$, $pK_2 = 8.88$ and $\alpha = 4.55$. The solid lines in Fig.3-5 are regression curves.

These results indicate that the complex formation of protein with Co(0) promotes the tendency of the ionizable group to be deprotonated

and that the catalytic activity of protein-S⁻-Co(0) complex is larger than that of protein-SH-Co(0). The value of pK_1 obtained here may correspond with the sulfphydry group's pK of adsorbed RNase, but is slightly higher than pK of sulfhydryl group of cysteine molecule in solution ($pK = 8.33^{42}$).

Effect of Temperature:

Fig.3-7 shows d.c. polarograms of $4 \mu\text{g cm}^{-3}$ RNase at 10, 25, and 40 °C in the base solution of $0.1 \text{ mol dm}^{-3} \text{NH}_3$, $0.1 \text{ mol dm}^{-3} \text{NH}_4\text{Cl}$ and $0.1 \text{ mol dm}^{-3} \text{KCl}$ containing $2 \times 10^{-4} \text{ mol dm}^{-3} \text{Co(III)}$ and broken lines represent polarograms in the absence of RNase at corresponding temperature. The diffusion current of cobalt ion increases with temperature, because of the increase in the diffusion coefficient of cobalt ion. The Brdicka currents at -1.3, -1.4 and -1.5 V are plotted against temperature in Fig.3-8. The value of $i_B(-1.3 \text{ V})$ increases with temperature from 10 to 30 °C but above 30 °C $i_B(-1.3 \text{ V})$ decreases with temperature. The values of $i_B(-1.4 \text{ V})$ and $i_B(-1.5 \text{ V})$ decrease monotonously with temperature in the temperature range investigated. This behavior had been reported by many workers.^{30,37-39,43)} As previously

described, the Brdicka current is a function of Γ and f_{Co} , which are also the function of temperature. Then, we corrected the temperature effect

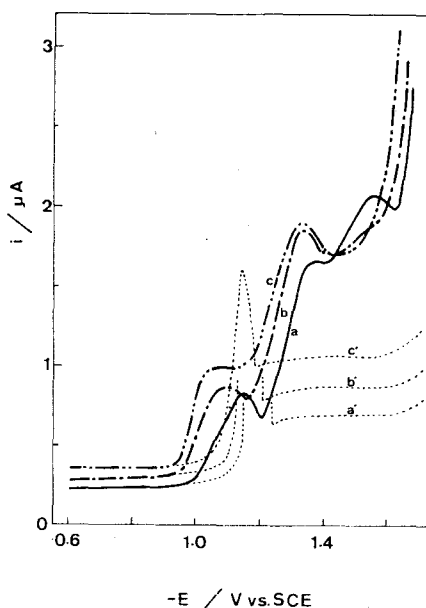


Fig.3-7. D.c. polarograms of $4 \mu\text{g cm}^{-3}$ RNase in 0.2 mol dm^{-3} ammoniacal buffer containing $2 \times 10^{-4} \text{ mol dm}^{-3} \text{Co(III)}$ at a) 10, b) 25, and c) 40 °C. (Broken lines represent d.c. polarograms in the absence of RNase at a') 10, b') 25, and c') 40 °C.)

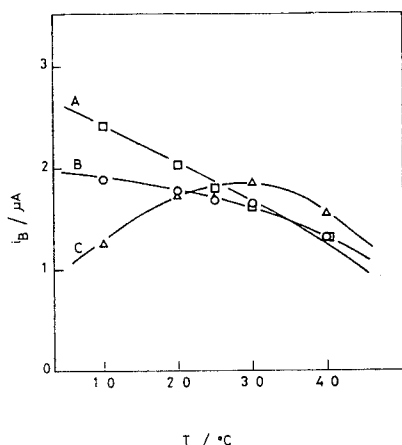


Fig.3-8. Temperature dependence of the Brdicka current of $4 \mu\text{g cm}^{-3}$ RNase in 0.2 mol dm^{-3} Co(III) at A) -1.5, B) -1.4 and C) -1.3 V.

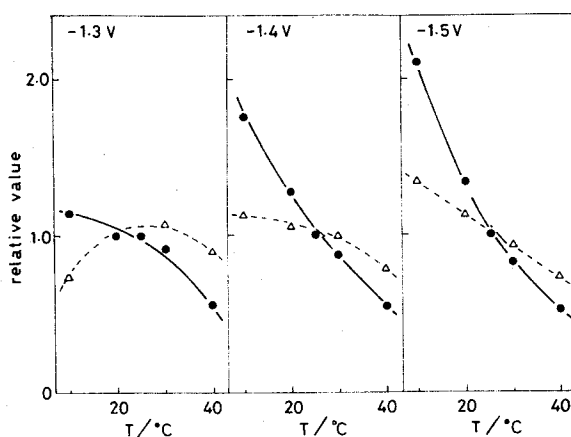


Fig.3-9. Temperature dependence of relative values of the Brdicka current (Δ) and the Brdicka current constant k_B (\bullet); data expressed as relative value to the value obtained at 25°C .

on Γ and f_{Co} . The f_{Co} value at a given temperature was estimated from the diffusion current of cobalt ion according to Ilkovic equation (broken lines in Fig.3-7). If the adsorption process is controlled by diffusion, the temperature effect of Γ is reduced to that of D_p , according to Koryta equation. The value of D_p were calculated using the relation⁴⁴⁾ $D_p(T) = (\text{const.})T/\eta(T)$, where $D_p(T)$ and $\eta(T)$ are diffusion coefficient of protein and viscosity of water at $T^\circ\text{K}$, respectively.

The relative values of k_B at a given temperature to that obtained at 25°C are plotted against temperature as shown in Fig.3-9. The values of k_B decrease monotonously with increasing temperature in the temperature range investigated at all the measurement potentials. Although Brezina and Gultja⁴¹⁾ attributed an increase in the first wave height with temperature to an increase in reaction rate of catalytic active complex formation, above results indicate that the apparent increase in i_B (-1.3 V) from 10 to 30°C is attributed to the increase in f_{Co} and/or Γ with temperature.

We also determined the $n_c k_c$ and k_f/k_d values at various temperature. Fig.3-10 shows the dependence of $n_c k_c$ on temperature. The value of $n_c k_c$ increases with increasing temperature at all the measurement potential. Fig.3-11 shows the temperature dependence of k_f/k_d . The k_f/k_d value decreases with temperature. In other words, the intrinsic catalytic activity of protein-Co(0) complex increases with temperature, but in contrast, the complex becomes less stable or the surface concentration of the complex decreases with temperature. Many investigators^{30,38,43} suggested that negative temperature effect of the Brdicka current is attributed to the desorption of protein. However, Γ must depend positively on temperature, because the adsorption is controlled by diffusion under these conditions. The results described here indicate that the monotonous decrease in over-all catalytic activity constant k_B is attributed to the decrease in the stability of protein-Co(0) complex.

The slope of linear lines in Fig.3-10 give the apparent activation energy of the hydrogen evolution reaction on electrode surface, $(E^a)_{app}$.

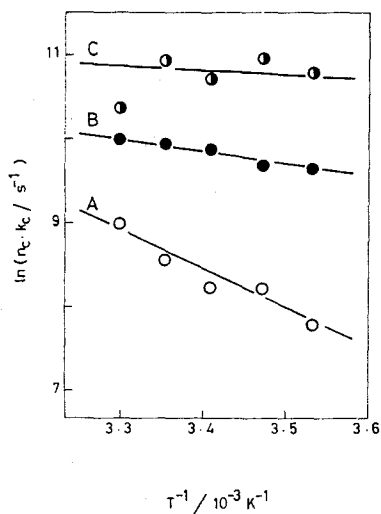


Fig.3-10. Dependence of $n_c k_c$ on temperature at A) -1.3, B) -1.4, and C) -1.5 V; data obtained in 0.2 mol dm^{-3} ammoniacal buffer containing $4 \text{ } \mu\text{g cm}^{-3}$ RNase.

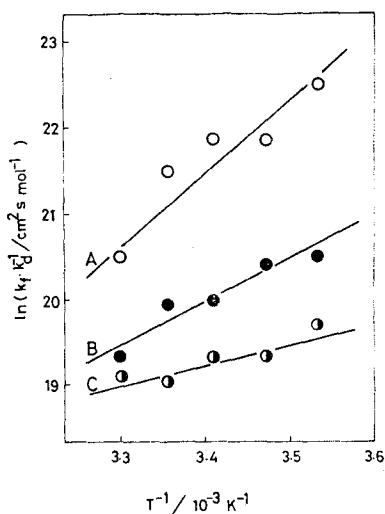


Fig.3-11. Dependence of k_f/k_d on temperature at A) -1.3, B) -1.4, and C) -1.5 V; data obtained in 0.2 mol dm^{-3} ammoniacal buffer containing $4 \text{ } \mu\text{g cm}^{-3}$ RNase.

These values were $(E^a)_{app}$ (at -1.3 V) = 12 kcal mol⁻¹, $(E^a)_{app}$ (at -1.4 V) = 5 kcal mol⁻¹ and $(E^a)_{app}$ (at -1.5 V) = 1 kcal mol⁻¹, indicating the almost linearly decrease in $(E^a)_{app}$ with negatively increasing potential.

The interpretation of the effect of temperature on the Brdicka current or the apparent activation energy of the hydrogen evolution reaction is complicated by the temperature effect of pH of ammoniacal buffer.⁴⁵⁾ In order to analyze strictly the effect of temperature on $n_c k_c$, the change in pH due to the temperature change has to be taken into consideration. We tried to correct pH effect using the relation,

$$\partial(n_c k_c)/\partial T = (\partial(n_c k_c)/\partial pH)_T (dpH/dT) + (\partial(n_c k_c)/\partial T)_{pH} \quad (3-12)$$

where $(\partial(n_c k_c)/\partial pH)_T$ was estimated tentatively from the $(n_c k_c)_0$ vs. pH plot in Fig.3-5 and $dpH/dT = -0.0303$ in the ammoniacal buffer at 25 °C.⁴⁶⁾ The corrected activation energy, $(\partial(n_c k_c)/\partial T)_{pH}$, at -1.4 V was estimated to be 7 kcal mol⁻¹.

SUMMARY

Effects of ammonia buffer concentration, C_{amm} , pH and temperature on $n_c k_c$ and k_f/k_d have been investigated. The dependence of $n_c k_c$ on C_{amm} indicates that water molecule as well as ammonium ion participates in the catalytic reaction as a proton donor. The k_f/k_d value slightly decreases with C_{amm} , suggesting participation of ammonia molecule in the protein-Co(0) complex formation. The sigmoidal pH-dependence has been found for $n_c k_c$ and k_f/k_d values corrected for the effect of buffer salts. This has been interpreted as due to the ionization of functional group (probably sulfhydryl group) in adsorbed protein. With increasing temperature, the $n_c k_c$ value increases, but k_f/k_d value decreases. The decrement of k_f/k_d is larger than the increment of $n_c k_c$, resulting in the decrease in overall catalytic activity with temperature. The apparent activation energy of the electrochemical hydrogen evolution has been estimated.

CHAPTER 4. PULSE POLAROGRAPHIC STUDIES ON BRDICKA CURRENT^{f)}

Pulse polarographic techniques were first introduced by Barker⁴⁷⁾ and now two types of the techniques, *i.e.* normal pulse polarography (NPP) and differential pulse polarography (DPP) are used. NPP is well suited to the study of the electrode process involving adsorption of proteins, since the electrode potential, on which the adsorption may be dependent, can be controlled stepwise. On the other hand, DPP is nowadays the most widely used polarographic technique for trace analysis, because DPP shows an improved sensitivity due to the better resolution of the current-voltage curves at very low concentration. In this chapter, the author investigated the characteristics of Brdicka current in NPP and DPP on the basis of the theoretical equation described in chapter 1.

EXPERIMENTAL

Materials:

Streptomyces subtilisin inhibitor (SSI) was a gift of Prof. K.Hiromi. Other chemicals used were described in chapter 2.

Apparatus:

Normal pulse (NP)-, differential pulse (DP)- and d.c.-polarograms were recorded with Yanagimoto voltammetric analyzer P-1000, equipped with Watanabe X-Y recorder WX-4401. Characteristics of a dropping mercury electrode (dme) were $m = 0.852 \text{ mg s}^{-1}$ and $t = 11.08 \text{ s}$ at mercury reservoir height $h = 50.0 \text{ cm Hg}$ at $E = -1.5 \text{ V}$ in an ammoniacal buffer. Drop time was regulated usually at $\tau = 1.67 \text{ s}$. In NP polarographic mode, a series of increasing amplitude voltage pulses starting from an initial potential, E_i^{NP} , were imposed on successive drops at the end of drop life. The potential pulse is of 50 ms duration. The current was sampled over a

16.6 ms interval toward the end of the pulse duration. In DP polarographic mode, small finite amplitude (ΔE_p^{DP}) pulses of 50 ms duration, superimposed on a conventional d.c. ramp voltage, are applied to the dme near to the end of drop life time. The current output is amplified at two time intervals (16.6 ms); immediately on the ramp prior to the imposition of the pulse and then again at the end of the pulse. The difference in these two currents is displayed.

Electrochemical Measurements:

All of electrochemical measurements were described in chapter 2.

EQUATIONS OF BRDICKA CURRENT IN PULSE POLAROGRAPHY

NORMAL PULSE POLAROGRAPHIC BRDICKA CURRENT

In chapter 1, the author showed that the Brdicka current in d.c. polarographic mode can be well explained by Eq.(1-4) at relatively low concentration of cobalt ion. In NP polarographic mode, protein is adsorbed at a given initial potential E_i^{NP} , and cobalt ion should be preelectrolyzed at a certain E_i^{NP} . If the adsorption of protein on mercury electrode is strong at E_i^{NP} and the adsorption and/or desorption are negligibly small during the pulse duration, Γ can be estimated by Eq.(1-10) and is independent of E_i^{NP} and E_m . When we use Co(III), electrochemical state of cobalt during the preelectrolysis is Co(III), Co(II) or Co(0) depending on E_i^{NP} . Then, the flux of cobalt ion at the electrode surface, f_{Co}^{NP} on pulse imposition is generally expressed by

$$f_{Co}^{NP} = f_{Co(III)}^{NP} + f_{Co(II)}^{NP} \quad (4-1)$$

The value of f_{Co}^{NP} can be evaluated in three different E_i^{NP} regions for the

case of Co(III) ion. At the E_i^{NP} value more positive than the reduction potential of Co(III) to Co(II), $f_{Co(III)}^{NP}$, can be given by Cottrell equation,

$$f_{Co(III)}^{NP} = (D_{Co}/\pi t_p)^{1/2} C_{Co(III)} \quad (4-2)$$

and $f_{Co(II)}^{NP} = 0$, where t_p is the pulse duration time. Note that $f_{Co(III)}^{NP}$ is about 5 to 10 times larger than $f_{Co(III)}^{DC}$ expressed by Eq.(1-6). Second; in the E_i^{NP} region of the limiting current of Co(III) to Co(II) reduction, where Co(III) ion concentration near the electrode surface is depressed and Co(II) ion is generated by preelectrolysis at E_i^{NP} , $f_{Co(III)}^{NP}$ is given by Ilkovic equation (Eq.(1-6)) and $f_{Co(II)}^{NP}$ is given, from the theory of reverse pulse polarography,⁴⁸⁾ by

$$f_{Co(II)}^{NP} = (7D_{Co}/3\pi t_p)^{1/2} ((3\pi/7t_p)^{1/2} - 1) C_{Co(III)} \quad (4-3)$$

Note that sum of $f_{Co(II)}^{NP}$ and $f_{Co(III)}^{NP}$ in Eqs.(4-3) and (1-6) are equal to Cottrell equation (Eq.(4-2)). Third; in the E_i^{NP} region of the limiting current of Co(II) to Co(0), $f_{Co(III)}^{NP}$ is given by Ilkovic equation (Eq.(1-6)). Under these conditions, the difference in Brdicka currents in NP- and d.c.-polarographic mode should be attributed to the difference in the adsorption potential of protein.

Because the Brdicka current activity constant of Co(II), $k_{B,Co(II)}$, is different from that of Co(III), $k_{B,Co(III)}$, as described in chapter 2, NP polarographic Brdicka current at extremely low concentration of Co(III) can be expressed by

$$i_{B,C_{Co(III)} \rightarrow 0}^{NP} = FA\Gamma(k_{B,Co(II)} f_{Co(II)}^{NP} + k_{B,Co(III)} f_{Co(III)}^{NP}) \quad (4-4)$$

DIFFERENTIAL PULSE POLAROGRAPHIC BRDICKA CURRENT

When the drop time, τ , is long in comparison with the pulse duration, t_p , the electrode surface area, A , is practically constant during the

first and second current sampling or at $\tau - t_p$ and τ in DP polarographic mode. In the limiting current region of Co(II) to Co(0) , the f_{Co} in DP polarographic mode, $f_{\text{Co}}^{\text{DP}}$, is also practically constant at $\tau - t_p$ and τ , and given by Ilkovic equation. Further, if protein is adsorbed strongly on electrode surface and we can neglect the desorption of protein during the small amplitude (ΔE_p^{DP}) imposition, Γ is practically constant at $\tau - t_p$ and τ , and given by Koryta equation. Then, the Brdicka current in DP polarographic mode at small ΔE_p^{DP} and extremely low C_{Co} can be expressed by

$$\begin{aligned}
 i_{B, C_{\text{Co}} \rightarrow 0}^{\text{DP}} &= i_B(E_m - \Delta E_p^{\text{DP}}, \tau) - i_B(E_m, \tau - t_p) \\
 &\approx i_B(E_m - \Delta E_p^{\text{DP}}, \tau) - i_B(E_m, \tau) \\
 &\approx \frac{di_B(E_m, t)}{dE_m} \Delta E_p^{\text{DP}} \\
 &\approx FA\Gamma f_{\text{Co}}^{\text{DP}} \frac{dk_B(E_m)}{dE_m} \Delta E_p^{\text{DP}}
 \end{aligned} \tag{4-5}$$

RESULTS AND DISCUSSION

NORMAL PULSE POLAROGRAPHIC BRDICKA CURRENT

Fig.4-1 shows normal pulse (NP) polarogram of SSI in the base solution containing $2 \times 10^{-4} \text{ mol dm}^{-3}$ hexaaminecobalt (III) chloride, Co(III) , as well as d.c. polarogram. The second wave of Brdicka current is higher than the first one on the NP polarogram, contrary to the d.c. polarogram. In the following, we shall discuss the NP Brdicka current at -1.4 and -1.6 V, $i_B^{\text{NP}}(-1.4 \text{ V})$ and $i_B^{\text{NP}}(-1.6 \text{ V})$, corresponding to the first and second Brdicka waves, respectively.

We investigated the dependence of $i_B^{\text{NP}}(-1.4 \text{ V})$ and $i_B^{\text{NP}}(-1.6 \text{ V})$ on

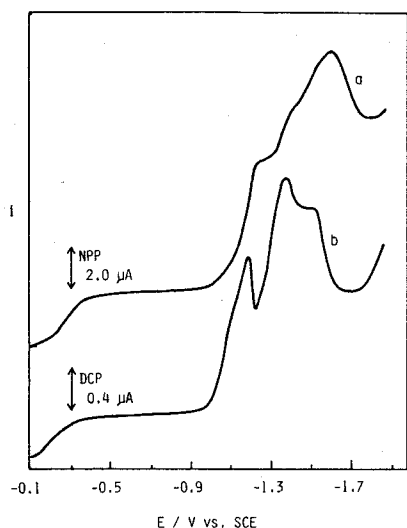


Fig.4-1. (a) Normal pulse polarogram and (b) d.c. polarogram of $2 \mu\text{g cm}^{-3}$ SSI in ammoniacal base solution (pH 10.0) containing $2 \times 10^{-4} \text{ mol dm}^{-3} \text{ Co(III)}$.

the drop time, τ , at $h = 36.6 \text{ cm Hg}$ and $\tau = 0.85$ to 8.25 s , and on the mercury reservoir height, h , at $\tau = 1.67 \text{ s}$ and $h = 17.8$ to 81.3 cm Hg , both at $C_{\text{Co(III)}} = 2 \times 10^{-5} \text{ mol dm}^{-3}$ and $E_i^{\text{NP}} = -0.1 \text{ V}$. Table 4-1 shows the results: the exponent x and y in the expression of $i_B^{\text{NP}} = (\text{const.})\tau^x$ and $i_B^{\text{NP}} = (\text{const.})h^y$, respectively. At $E_i^{\text{NP}} = -0.1 \text{ V}$, $f_{\text{Co(III)}}^{\text{NP}}$ is given by Eq.(4-2) and $f_{\text{Co(II)}}^{\text{NP}} = 0$. Then, from Eqs.(1-10), (4-2) and (4-4), x and y are expected to be $7/6$ and $2/3$, respectively. Note that $A = (\text{const.})\tau^{2/3}$ at constant h , and $A = (\text{const.})h^{2/3}$ at constant τ . The values in Table 4-1 are in accordance with the theoretical value within the experimental error, taking into account that both values of x and y for the cobalt limiting diffusion current in NP polarographic mode, $i_{\text{Co}}^{\text{NP}}$, in Table 4-1 are theoretically expected to be $2/3$.

The values of $i_B^{\text{NP}}(-1.4 \text{ V})$, $i_B^{\text{NP}}(-1.6 \text{ V})$ increased linearly with the protein concentration, C_p , up to $60 \mu\text{g cm}^{-3}$ at $E_i = -0.1 \text{ V}$ and $\tau = 1.67 \text{ s}$: the result is well explained by Eqs.(4-4) and (1-10). The i_B^{NP} first increased with the cobalt concentration, $C_{\text{Co(III)}}$, and showed a parabolic dependence on $C_{\text{Co(III)}}$ at higher $C_{\text{Co(III)}}$. The linear relationship held up to $C_{\text{Co(III)}} = 2 \times 10^{-6} \text{ mol dm}^{-3}$ for $i_B^{\text{NP}}(-1.4 \text{ V})$ and $1.5 \times 10^{-5} \text{ mol dm}^{-3}$ for $i_B^{\text{NP}}(-1.6 \text{ V})$ is well explained by Eqs.(4-2) and (4-4). The upper limit of linear relation between i_B^{NP} and $C_{\text{Co(III)}}$ is about one tenth of

Table 4-1. Dependence of Normal- and Differential-Pulse Polarographic Brdicka Currents and Cobalt Reduction Currents on the Drop Time and the Mercury Reservoir Height.

Method	Current	x ¹⁾	y ²⁾
NPP	$i_B^{NP} (-1.4V)$	1.1	0.80
	$i_B^{NP} (-1.6V)$	1.1	0.78
	i_{Co}^{NP}	0.76	0.78
DPP	$i_B^{DP} (I)$	0.73	0.76
	$i_B^{DP} (II)$	0.83	0.74
	i_{Co}^{DP}	0.34	0.78

1) Expressed in $i = (\text{const.})\tau^x$ at constant h .

2) Expressed in $i = (\text{const.})h^y$ at constant τ .

the case in d.c. polarography. This result can be explained by the dependence of i_B on f_{Co} as expressed by Eq.(1-2) and the fact that $f_{Co(III)}^{NP}$ expressed by Eq.(4-2) is about ten times larger than $f_{Co(III)}^{DC}$ expressed by Eq.(1-6). From above results, the Brdicka current in NP polarographic mode is fundamentally expressed by Eq.(4-4) at the low concentration of cobalt ion.

E_i^{NP} Dependence of i_B^{NP} :

The Brdicka current in NPP was dependent on the initial potential. E_i^{NP} . Fig.4-2 shows the i_B^{NP} (-1.4 V) and i_B^{NP} (-1.6 V) plotted against E_i^{NP} . The i_B^{NP} values first decreased with decreasing E_i^{NP} from -0.1 V to -0.4 V, second, became constant from $E_i^{NP} = -0.4$ V to -0.9 V where wave form was independent of E_i^{NP} , third, decreased again with the decreasing E_i^{NP} from -0.9 V to -1.2 V, and finally became constant within the potential range of $E_i^{NP} = -1.2$ V to -1.4 V.

The first decrease in i_B^{NP} around -0.2 V, where the reduction of Co(III) to Co(II) begins, should be attributed to the decrease in $f_{Co(III)}^{NP}/f_{Co(II)}^{NP}$, because k_B value of Co(II), $k_{B,Co(II)}$, is smaller than that of Co(III), $k_{B,Co(III)}$, as described in chapter 2 and the decrease in i_B^{NP} in this E_i^{NP} region was not observed on using Co(II) instead of Co(III). In the E_i^{NP} region from -0.4 V to -0.9 V (constant current region), adsorption of protein is very strong^{12,16,26} and is independent of E_i^{NP} , and $f_{Co(II)}^{NP}$ and $f_{Co(III)}^{NP}$ are given by Eqs.(4-3), (1-6), respectively,

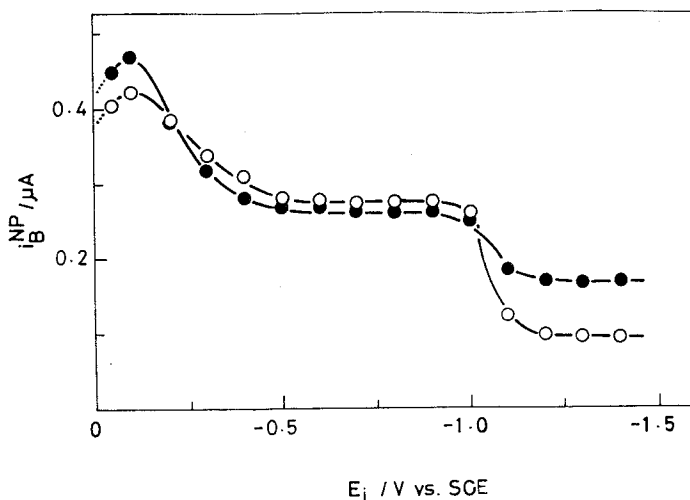


Fig.4-2. Initial potential dependence of normal pulse polarographic Brdicka current at $E_m = -1.4$ V (O) and -1.6 V (●); data obtained in the ammoniacal base solution (pH 9.5) containing $4 \mu g cm^{-3}$ SSI and $3 \times 10^{-5} mol dm^{-3}$ Co(III).

and are also independent of E_i^{NP} . Then, i_B^{NP} is expected to be independent of E_i^{NP} , according to Eq.(4-4).

Here we shall discuss $k_{B,Co(II)}$ and $k_{B,Co(III)}$. From above discussions (see Eqs.(1-6), (4-2), (4-3), (4-4)), the ratio of NP polarographic Brdicka currents at $E_i^{NP} = -0.5$ V to that at $E_i^{NP} = -0.1$ V can be expressed by

$$\frac{i_B^{NP}(E_i^{NP} = -0.5 \text{ V})}{i_B^{NP}(E_i^{NP} = -0.1 \text{ V})} = \frac{k_{B,Co(II)}}{k_{B,Co(III)}} \left(1 - \sqrt{\frac{7t_P}{3\tau}}\right) + \frac{7t_P}{3\tau} \quad (4-6)$$

According to Eq.(4-6), we tried to evaluate $k_{B,Co(II)}/k_{B,Co(III)}$ from $i_B^{NP}(E_i^{NP} = -0.5 \text{ V})/i_B^{NP}(E_i^{NP} = -0.1 \text{ V})$ at $\tau = 1.67$ and 8.25 s. The results are $k_{B,Co(II)}/k_{B,Co(III)}$ (at -1.4 V) = 0.65 at $\tau = 1.67$ s and 0.67 at $\tau = 8.25$ s, and $k_{B,Co(II)}/k_{B,Co(III)}$ (at -1.6 V) = 0.43 at $\tau = 1.67$ s and 0.43 at $\tau = 8.25$ s. The $k_{B,Co(II)}/k_{B,Co(III)}$ (at -1.4 V) estimated by above method is in agreement with the value estimated by d.c. polarographic method ($= 0.69/1.2 = 0.58$, see Table 2-1) within experimental error. These results indicate the validity of the theory, and that k_B is dependent on the measurement electrode potential, but not E_i^{NP} .

Although the disulfide groups in protein should be reduced around -0.75 V at pH 9.5,^{49,50)} the k_B value was independent of E_i^{NP} at least from -0.4 V to -0.9 V. This result indicates that the adsorption state or electrochemical state of proteins on electrode surface at initial potential before the pulse imposition scarcely, if any, affect the k_B value or the Brdicka current in NP polarographic mode.

The decrease in i_B^{NP} around $E_i^{NP} = -1.1$ V had previously been reported by Palecek *et al.*⁵¹⁾ They suggested that this phenomenon was attributed to the conformational change of adsorbed protein. However, this phenomenon around $E_i^{NP} = -1.1$ V, where the reduction of Co(II) to Co(0) becomes appreciable, should be attributed to the decrease in the flux of cobalt ion (compare Eq.(1-6) with Eq.(4-2)).

Fig.4-3 shows the NP polarographic Brdicka waves at various E_i^{NP}

more negative than -1.3 V and at $C_{\text{Co(III)}} = 2 \times 10^{-4} \text{ mol dm}^{-3}$, in contrast to the d.c. polarographic Brdicka wave (broken line). Under these conditions, Co(III) ion near the electrode surface is preelectrolyzed to Co(0) before the pulse imposition and the flux of cobalt ion in NP polarographic mode is equal to that in d.c. polarographic mode. On the other hand, protein is adsorbed at E_i^{NP} in NP polarography, but at the measurement potential E_m in d.c. polarography. When E_i^{NP} is less negative than -1.4 V, i_B^{NP} is nearly equal to i_B^{DC} at E_m less negative than -1.4 V; under these conditions the second Brdicka wave is larger than the first wave in NP polarogram contrary to d.c. polarogram (see also Fig.4-1). When E_i^{NP} is more negative than -1.45 V, i_B^{NP} decreases sharply with negatively increasing E_i^{NP} , in accordance with the sharp decrease in d.c. polarographic wave, though i_B^{NP} is larger than i_B^{DC} . These facts indicate that the adsorption of SSI at the potential less negative than -1.4 V is very strong and irreversible; the SSI molecule adsorbed at less negative potential than -1.4 V is hardly desorbed on the duration of more negative potential pulse, and that the adsorptivity becomes to decrease with negatively increasing the electrode potential than -1.4 V. The shape of ordinary d.c. polarographic Brdicka wave is determined by the potential dependence of k_B and Γ , and the shape of NP polarographic Brdicka wave is determined mainly by the potential dependence of k_B . The appearance of the double wave in NP polarogram

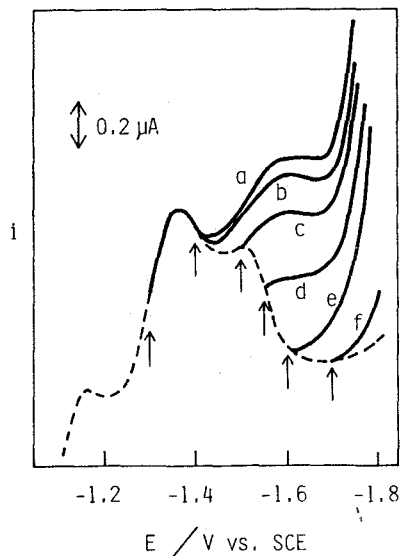


Fig.4-3. Initial potential dependence of normal pulse polarogram of $2 \mu\text{g cm}^{-3}$ SSI in ammoniacal base solution containing $2 \times 10^{-4} \text{ mol dm}^{-3}$ Co(III). $E_i^{\text{NP}} =$ a) -1.3 V, b) -1.4 V, c) -1.5 V, d) -1.55 V, e) -1.6 V, and f) -1.7 V. Broken line represents d.c. polarogram recorded in the same sample solution.

(or the dependence of k_B on the electrode potential) suggests a very large conformational change of adsorbed SSI molecule at about -1.45 V.

DIFFERENTIAL PULSE POLAROGRAPHIC BRDICKA CURRENT

Fig.4-4 shows differential pulse (DP) polarogram of SSI in the base solution containing $2 \times 10^{-4} \text{ mol dm}^{-3} \text{ Co(III)}$, as well as d.c. polarogram. The Brdicka wave on DP polarogram is almost a differential form of d.c. polarographic Brdicka wave (see below). The first peak of DP polarogram is higher than the second one, in good accordance with the relation of the heights of both d.c. polarographic waves. In the following current measurement, difference between the current of the first peak (at about -1.3 V) or the second peak (at about -1.5 V) and the current of the hollow (at about -1.4 V) was measured and represented as $i_B^{\text{DP}}(\text{I})$ or $i_B^{\text{DP}}(\text{II})$, respectively.

The peak heights of DP polarographic Brdicka current, $i_B^{\text{DP}}(\text{I})$ and $i_B^{\text{DP}}(\text{II})$, increase linearly with the pulse amplitude, ΔE_P^{DP} , up to -50 mV, and tend to level off at higher ΔE_P^{DP} (Fig.4-5). The linearity between i_B^{DP} and ΔE_P^{DP} can be well explained by Eq.(4-5). The peak potentials of the first peak, $E_P^{\text{DP}}(\text{I})$, and the second peak, $E_P^{\text{DP}}(\text{II})$, have a tendency to shift less negative with ΔE_P^{DP} , as well as the relation of cobalt reduction peak (Fig.4-6). The relation between $E_P^{\text{DP}}(\text{I})$ or $E_P^{\text{DP}}(\text{II})$ and ΔE_P^{DP} was empirically expressed by

$$E_P^{\text{DP}} = E_{P,0}^{\text{DP}} - \Delta E_P^{\text{DP}}/2 \quad (4-7)$$

where $E_{P,0}^{\text{DP}}$ is the extrapolated value of $E_P^{\text{DP}}(\text{I})$ $2 \times 10^{-4} \text{ mol dm}^{-3} \text{ Co(III)}$.

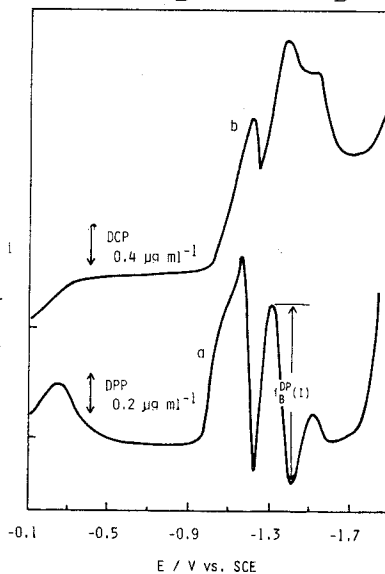


Fig.4-4 a) Differential pulse and b) d.c.polarograms of $2 \mu\text{g cm}^{-3}$ SSI in the base solution (pH 10.0) containing $2 \times 10^{-4} \text{ mol dm}^{-3} \text{ Co(III)}$.

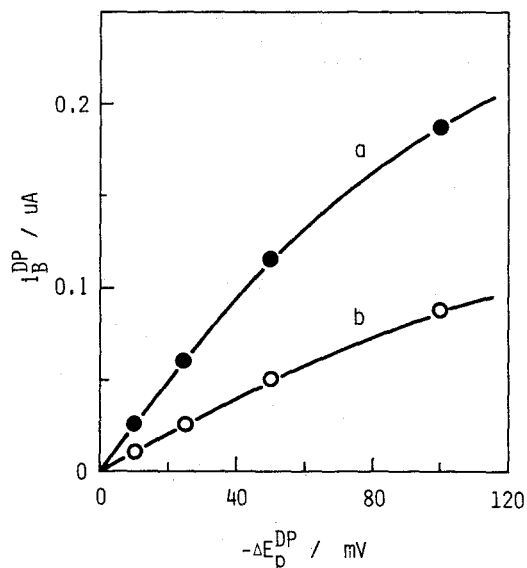


Fig.4-5 Pulse amplitude dependence of the first- (a) and second- (b) peak heights of differential pulse polarographic Brdicka current.

$C_{\text{SSI}} = 2 \mu\text{g cm}^{-3}$, $C_{\text{Co(III)}} = 5 \times 10^{-5} \text{ mol dm}^{-3}$, $\tau = 1.67 \text{ s}$, $h = 32.6 \text{ cmHg}$. the presence of SSI.

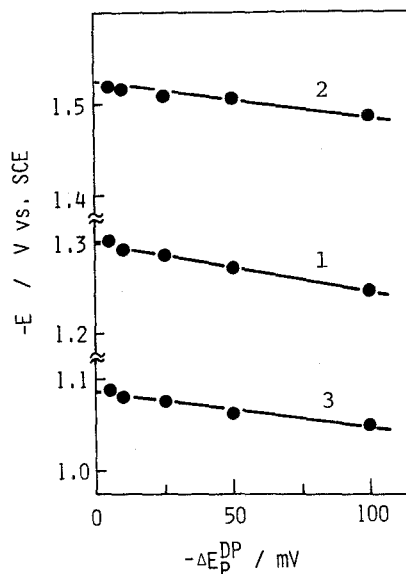


Fig.4-6 Plots of peak potential against pulse amplitude; 1) the first peak potential $E_p^{DP}(\text{I})$, 2) the second peak potential $E_p^{DP}(\text{II})$, 3) cobalt reduction potential in the presence of SSI.

or $E_p^{DP}(\text{II})$ to $\Delta E_p^{DP} = 0$. In the following, ΔE_p^{DP} was set to be -50 mV .

At constant mercury reservoir height ($h = 36.6 \text{ cm Hg}$), the dependence of $i_B^{DP}(\text{I})$ and $i_B^{DP}(\text{II})$ on the drop time was investigated in the drop time region of $\tau = 0.83$ to 8.25 s . Results are expressed by exponent x in $i_B^{DP} = (\text{const.})\tau^x$, and given in Table 4-1. We also investigated the mercury reservoir height dependence of i_B^{DP} at $\tau = 1.67 \text{ s}$ in the $h = 17.8$ to 81.3 cm Hg region. The results are given in Table 4-1, by the expression of exponent y in $i_B^{DP} = (\text{const.})h^y$. From Eqs.(1-6), (1-10) and (4-5), both x and y are expected to be $2/3$. The values in Table 4-1 are in agreement with the theoretical value within the experimental error, though the deviation of the experimental values for $i_B^{DP}(\text{II})$ from the theoretical values was larger than for $i_B^{DP}(\text{I})$.

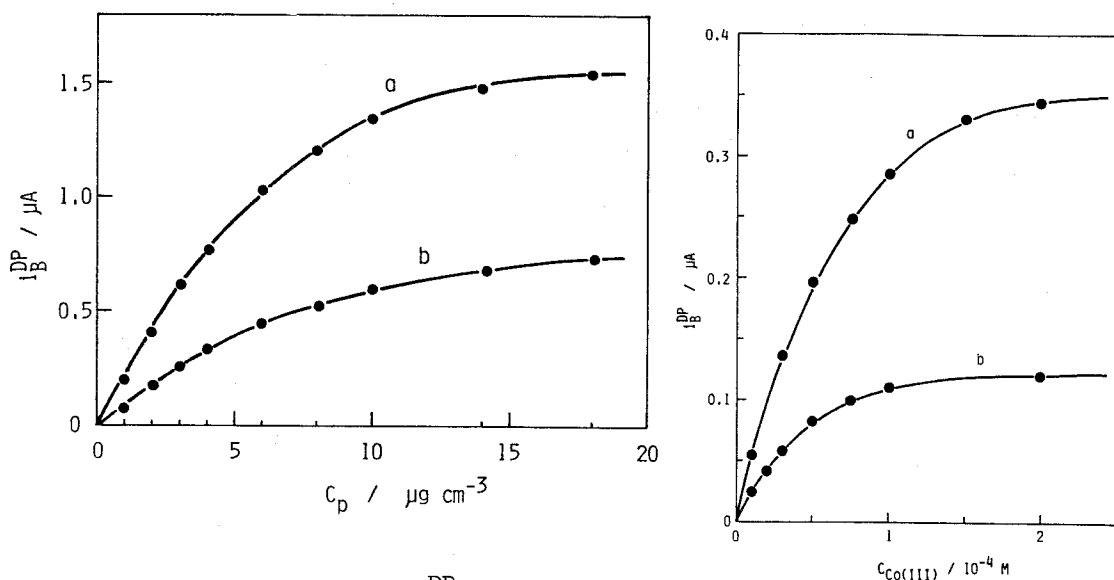


Fig.4-7 Dependence of a) i_B^{DP} (I) and b) i_B^{DP} (II) on the SSI concentration; data obtained at $\Delta E_P^{DP} = -50$ mV, $h = 50$ cm Hg, and b) i_B^{DP} (II) on $C_{Co(III)}$; $C_{Co(III)} = 2 \times 10^{-4}$ mol dm $^{-3}$, $v = 2$ mV s $^{-1}$. $C_{SSI} = 2$ μ g cm $^{-3}$.

Fig.4-7 shows the dependence of i_B^{NP} (I) and i_B^{DP} (II) on the protein concentration. The peak height, i_B^{DP} (I) and i_B^{DP} (II), increased linearly with the SSI concentration up to 4 μ g cm $^{-3}$, and tended to reach certain maximum values at higher concentration of SSI. The linear relation can be explained by Eqs.(1-10) and (4-5). The maximum value may be corresponded to the current at $\Gamma = \Gamma^{max}$. However, the highest C_p value in linear relation region was about one fourth of that in d.c. polarographic Brdicka current. This result can not be explained at the present time.

We also investigated the dependence of the concentration of Co(III), $C_{Co(III)}$, on i_B^{DP} (I) and i_B^{DP} (II). Fig.4-8 shows the result. The i_B^{DP} values increased at first linearly with $C_{Co(III)}$ up to 3×10^{-5} mol dm $^{-3}$ and parabolically at higher $C_{Co(III)}$. The linear relation between peak height and $C_{Co(III)}$ is predicted by Eqs.(1-6) and (4-5). In conclusion, the above results indicate that the DP polarographic Brdicka current can be fundamentally expressed by Eq.(4-5).

Here we tried to calculate the difference in d.c. polarographic current at the potentials E and $E + \Delta E$, $\Delta i^{DC} = i^{DC}(E + \Delta E) - i^{DC}(E)$. The Δi^{DC} vs. E curve at $\Delta E = -50$ mV, calculated from the d.c. polarogram in Fig.4-4, was shown in Fig.4-9 (curve a). We also calculated the differential curve of d.c. polarogram by a numerical differentiation using a moving second order polynomial fit selecting five points as one set. Curve b in Fig.4-9 shows $(di^{DC}/dE)\Delta E$ vs. E curve at $\Delta E = -50$ mV. The Δi^{DC} vs. E curve and the $(di^{DC}/dE)\Delta E$ vs. E curve are nearly same shape, though the peak potential of Δi^{DC} vs. E curve is less negative by about 25 mV and peak height of Δi^{DC} is smaller than $(di^{DC}/dE)\Delta E$.

If Γ is independent of E and ΔE_P^{DP} is very small, Eq.(4-5) predicts that DP polarographic Brdicka current is almost equal to Δi^{DC} or $(di^{DC}/dE)\Delta E$. The real DP polarographic Brdicka wave at $\Delta E_P^{DP} = -50$ mV

as shown by broken line in Fig.4-9, was almost in agreement with Δi^{DC} vs. E curve or $(di^{DC}/dE)\Delta E$ vs. E curve in the potential range from -1.2 to -1.45 V, however, at more negative potential than -1.45 V, the deviation became large. These results show the following: at less negative potential than -1.45 V, the adsorption of SSI is strong and controlled by diffusion, then DP polarographic Brdicka current is, as a first

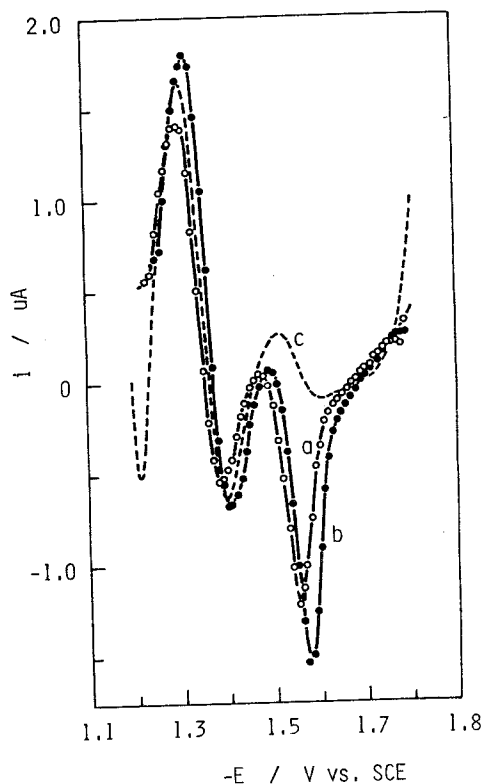


Fig.4-9 Plots of Δi^{DC} ($= i^{DC}(E + \Delta E) - i^{DC}(E)$) (○) and $(di^{DC}/dE)\Delta E$ (●) against E . Broken line represents differential pulse polarogram in Fig.4-4; data obtained from the d.c. polarogram in Fig.4-4 at $\Delta E = -50$ mV.

approximation, expressed by Eq.(4-5). With negatively increasing the potential, however, the adsorption becomes weak and Γ can no longer be estimated by Koryta equation and depends on the electrode potential, then i_B^{DP} deviates from the simple equation such as Eq.(4-5). This interpretation is in good agreement with the result of the initial potential dependence of NP polarographic Brdicka current described in previous section.

SUMMARY

On the basis of the basic equation of Brdicka current (chapter 1), theoretical equations of normal pulse (NP)- and differential pulse (DP)-polarographic Brdicka currents have been derived. These equations well explain the experimental results of NP- and DP-polarographic Brdicka currents.

Pulse polarographic study on Brdicka current has revealed that at the less negative potential than -1.4 V the protein SSI is adsorbed strongly and irreversibly on mercury electrode and the surface concentration is controlled solely by diffusion. At more negative potential than -1.5 V the adsorption of SSI becomes weak with increasing negative potential and the surface concentration is controlled by both diffusion and adsorption. The latter is dependent on the electrode potential.

PART II. ANALYTICAL APPLICATIONS OF BRDICKA CURRENT

Chapter 5. TRACE ANALYSIS OF PROTEINS BY DIFFERENTIAL PULSE POLAROGRAPHIC TECHNIQUE^{f)}

Differential pulse (DP) polarographic study on Brdicka current as described in chapter 4 has suggested that the polarographic technique based on Brdicka current may become a remarkably sensitive method for trace analysis of Brdicka active proteins. Palecek and co-workers^{52,53)} have applied DP polarographic method to the Brdicka current of proteins and shown that trace analysis of protein as low as 50 ng cm^{-3} can be determined DP polarographically. In this study the author has shown that trace amount of proteins as low as a few ng cm^{-3} can be determined using the DP polarographic technique by selecting suitable experimental conditions. The result is described in this chapter.

EXPERIMENTAL

Electrochemical Measurements:

Apparatus of experiments has been described in chapter 4. On the basis of the results described in chapter 4, electrochemical measurements were done as follows. As the base solution, $0.2 \text{ mol dm}^{-3} \text{ NH}_3 - \text{NH}_4\text{Cl}$ buffer solution (pH 10.0) containing $2 \times 10^{-4} \text{ mol dm}^{-3} \text{ Co}(\text{NH}_3)_6\text{Cl}_3$ was used. The ionic strength of the base solution was adjusted to 0.2 mol dm^{-3} with KCl. Ten cm^3 of the base solution was transferred into a polarographic cell and deaerated by passing nitrogen gas through the base solution for 15 to 20 min unless otherwise stated. Then an aliquot of protein stock solution was introduced into the deaerated base solution with a microsyringe and the solution was stirred with a magnetic stirrer for 3 min. After solution was allowed to stand for 3 min, differential

pulse polarograms were recorded with sweep rate, $v = 1.0 \text{ mV s}^{-1}$, the pulse amplitude, $\Delta E_P^{\text{DP}} = -50 \text{ mV}$ and drop time, $\tau = 3.3 \text{ s}$. In the case of current measurements at a fixed potential, the current was recorded after enough time had elapsed from the memory circuits of the instrument to become fully charged^{54,55)} (more than 15 drops of Hg in our case). All measurements were made under nitrogen atmosphere at $25.0 \pm 0.5 \text{ }^\circ\text{C}$ in a thermostat.

RESULTS AND DISCUSSION

The differential pulse (DP) polarogram of SSI in the presence of Co(III) has been described in chapter 4. DP polarographic method is, generally, considered to be suitable for trace analysis, because the influence of depolarizers reduced at more positive potential is small at DP polarography than other method, *e.g.* d.c.polarography. For the purpose of trace analysis of proteins by DP polarographic Brdicka current, it is sufficient, in principle, that the output voltage representing the current in the catalytic current region is amplified. Fig.5-1A shows a DP polarogram of 50 ng cm^{-3} SSI recorded from $E_i^{\text{DP}} = -1.23 \text{ V}$, where the DP polarographic current of cobalt reduction becomes relatively small.

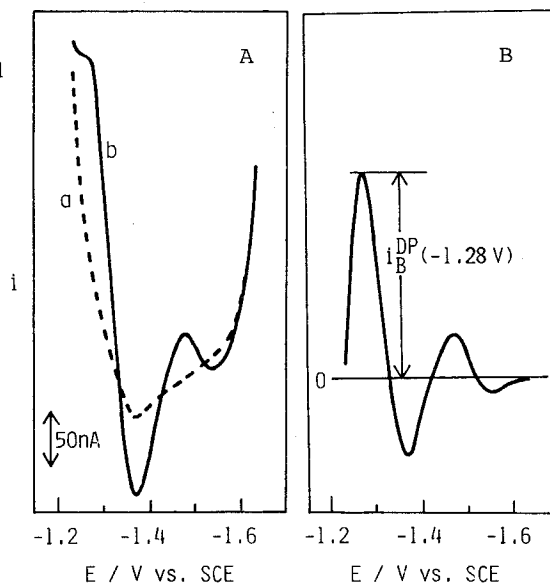


Fig.5-1 A) Differential pulse polarograms of a) the base solution and b) (a) + 50 ng cm^{-3} SSI. $E_i^{\text{DP}} = -1.23 \text{ V}$. B) Differential pulse Brdicka current *vs.* potential curve. The current was obtained by subtracting curve a from curve b in Fig.5-1A.

Fig.5-1B shows the DP polarographic Brdicka current, which is the current corrected for the base current (curve a in Fig.5-1A). DP polarographic Brdicka current has two peaks at about -1.3 and -1.5 V. Although, at lower protein concentration than 50 ng cm^{-3} , the first peak at positive potential was not very well defined in DP polarogram, but the increase in peak current with increasing SSI concentration was found to be more sensitive at the first peak than at the second peak, and the adsorption process of protein is more simple at less negative potential. Then we tried to perform amperometry at a fixed potential of E_{max} , which corresponds with the potential of the first peak of the DP polarographic Brdicka current. E_{max} was determined to be -1.28 V for SSI by manually recording the polarogram, according to Myers and Osteryoung.⁵⁵⁾ In determining the Brdicka current intensity, $i_B^{\text{DP}}(-1.28 \text{ V})$, the current was corrected for the base current (Method A). The value of $i_B^{\text{DP}}(-1.28 \text{ V})$ increased linearly with the protein concentration C_p from 40 ng cm^{-3} (Fig.5-2). At $C_p < 40 \text{ ng cm}^{-3}$, however, the calibration curve deviated upward from the straight line. We considered that the upward deviation of the calibration curve at low C_p is attributed to depression of protein in bulk solution due to the adsorption of protein on the glass wall of cell and/or the surface of electrolysis solution (air/water interface).

To prevent the depression of the protein of interest (in our case SSI), amperometry at the fixed potential ($E_m = -1.28 \text{ V}$) was performed under the conditions where 2 to $3 \mu\text{g cm}^{-3}$ of gelatine or α -amylase (*Bacillus subtilis*),⁵⁶⁾ which contains no SS, SH groups and are known to be Brdicka inactive protein, coexists in the base solution (Method B). The concentration of

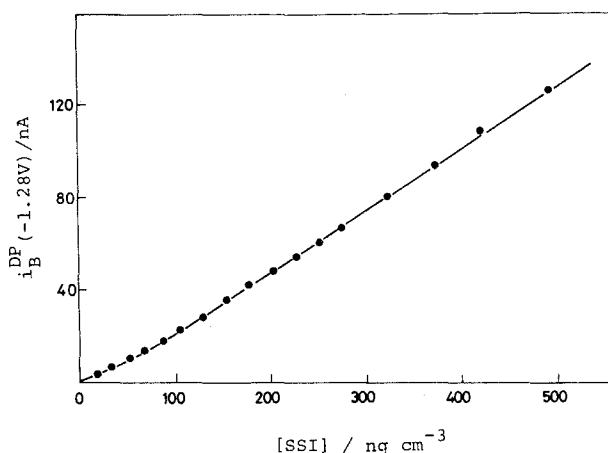


Fig.5-2 Calibration curve of SSI obtained by Method A (see text).

coexisting protein (e.g. α -amylase) was decided to be about 100 times larger than the intercept of extrapolation of the linear portion of calibration curve in Fig.5-2 to the adscissa, $C_P(i_B^{NP} \rightarrow 0) \approx 20 \text{ ng cm}^{-3}$, which should correspond to the amounts of protein adsorbed on solution/glass and/or solution/air interfaces. Under the conditions in Method B, the depression amount of the protein of interest due to the adsorption

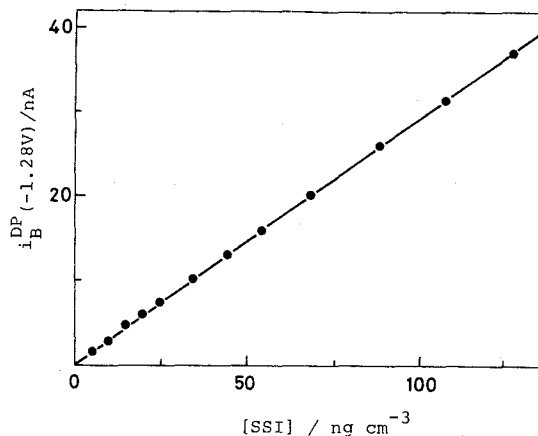


Fig.5-3 Calibration line of SSI obtained by Method B (see text).

should decrease to one hundredth of the case in Method A. The Brdicka current was corrected for the base current measured in the presence of α -amylase, though under these conditions, the change in the current due to the addition of α -amylase was merely recognizable. Fig.5-3 shows the calibration line of SSI in the presence of α -amylase for the coexisting protein. Good linear relation between $i_B^{DP}(-1.28 \text{ V})$ and C_P can be obtained in the C_P range from 5 to 2000 ng cm^{-3} . The correlation coefficient of the calibration line in Fig.5-3 was 0.9999. The resulting precision for replicate determination of SSI sample solution (5 times) was 1.73 % of coefficient of variation at $C_P = 51.1 \text{ ng cm}^{-3}$. The sensitivity of our method is much higher than that of the most often used methods of estimation of proteins such as a color reaction based on the Folin-Ciocalteu phenol reagent or the biuret reagent and estimation of proteins on the basis of absorption of UV light, i.e. the order of 1 to 1000 $\mu\text{g cm}^{-3}$.^{57,58)} Radio isotope method and fluorescence technique are also known to be trace analysis of proteins.⁵⁸⁾ Our electroanalytical method does not have inconveniences arising from use of isotope, and is not subject to the interference from coloration or turbidity of sample solution.

This polarographic method based on the Brdicka current can not be

applied to the estimation of proteins having no SH, SS group nor heme group, which becomes, contrarily, advantageous in preventing the adsorption of the protein of interest by coexisting such Brdicka-inactive proteins.

We also attempt the amperometric analysis under non-deaerated conditions (Method C), because the peak potential of oxygen reduction is less negative by about 0.3 V than the potential of the first peak (-1.28 V) and then effect of reduction current of oxygen in DP polarography should be much less than in d.c. polarography. Linear relationship between i_B^{DP} (-1.28 V) and C_p in the C_p range from 0.2 to 2.0 $\mu\text{g cm}^{-3}$ could be obtained. Detection of SSI as low as 20 ng cm^{-3} was also successful by this procedure (*i.e.* Method C), though the calibration curve at $C_p = 20$ to 200 ng cm^{-3} was slightly bent upward and the signal to noise ratio was less than that of Method A or B. From the view of the considerable saving in effort, Method C may offer a useful analytical method of proteins in very small amount of the base solution less than 1 cm^3 and/or in continuous sample treatment.⁵⁹⁾

We applied this DP polarographic analysis of proteins based on Brdicka current to the determination of the enzyme-inhibitor complex dissociation constant as low as 10^{-10} mol dm^{-3} and to the study on antigen-antibody interaction, as described in the following chapters.

SUMMARY

Differential pulse (DP) polarographic technique based on Brdicka current has been developed. Amperometry has been performed by applying a fixed potential of E_{max} (= -1.28 V), which corresponds with the potential of the first maximum of the DP polarographic Brdicka current of the protein. The Brdicka current at E_{max} is linearly depends on the protein concentration in the range between 3 $\mu\text{g cm}^{-3}$ and 5 ng cm^{-3} . Amperometry under non-deaerated conditions has also been studied, in which protein as low as 20 ng cm^{-3} can be detected.

Chapter 6. POLAROGRAPHIC STUDY ON ENZYME-INHIBITOR INTERACTION^{g,h,i)}

Streptomyces subtilisin inhibitor (SSI)⁶⁰⁾ and plasminostreptin (PS)⁶¹⁾ are protein proteinase inhibitors of microbial origin. These inhibitors, both containing SS-groups, are known to consist of two identical subunits and are able to bind one molecule of subtilisin BPN' (S.BPN', EC 3.4.21.14) per one subunit of the inhibitor to form S.BPN'-inhibitor complexes.^{61,62)} The dissociation constants of the complexes are as low as 10^{-10} to 10^{-8} mol dm⁻³, and their accurate determination has been a subject of intense studies.^{63,64)} In this chapter the author reports some basic features of Brdicka currents of SSI and PS and present a novel method for direct determination of the dissociation constants of the enzyme-inhibitor complexes as low as 10^{-10} mol dm⁻³. In determining the dissociation constants the multiple equilibrium involving microscopically distinct forms of the complexes has been taken into account.

EXPERIMENTAL

Chemicals:

Lyophilized preparations of *Streptomyces* subtilisin inhibitor (SSI) and plasminostreptin (PS) were provided by Prof. S.Murao of Osaka Prefecture University and Prof. K.Hiromi of Kyoto University, and Dr. A. Kakinuma of Takeda Chemical Industries, Ltd., respectively. Subtilisin BPN' (S.BPN') was purchased from Sigma Chemical Co. (lot No. 67C-0003). The purity of the enzyme preparation was determined to be 80.5 % according to Inouye *et al*'s method.⁶⁵⁾ All chemicals were of reagent grade quality.

Apparatus:

D.c. polarograms were recorded with a Yanagimoto polarograph P-8 or with a Yanagimoto potentiostat PE21-TB2S equipped with a Yokogawa-Hewlett-Packard function generator 3310 B and a Yokogawa X-Y recorder 3077. Two dropping mercury electrodes (dme) were used. Their characteristics were $m = 0.447 \text{ mg s}^{-1}$ and $\tau = 8.59 \text{ s}$ at -0.7 V and $h = 90 \text{ cm Hg}$ for dme I and $m = 1.448 \text{ mg s}^{-1}$ and $\tau = 5.43 \text{ s}$ at -0.7 V and $h = 44.6 \text{ cm Hg}$ for dme II both in ammoniacal buffer. For recording d.c. polarographic waves, the drop time was regulated at 4.07 s , unless otherwise stated, with a Yanagimoto drop controller P-8-RT. Voltage sweep voltammograms on a hanging mercury drop electrode (hmde) were recorded with a Yanagimoto potentiostat PE21-TB2S equipped with a Yokogawa X-Y recorder 3077. A Metrohm mercury drop electrode E410 was used, its surface area being $0.0187 \pm 0.0003 \text{ cm}^2$. Differential pulse (DP) and fast polarograms were recorded with a Yanagimoto voltammetric analyzer P-1000, equipped with a Watanabe X-Y recorder WX-4401. The characteristics of dme were $m = 0.852 \text{ mg s}^{-1}$ and $\tau = 11.08 \text{ s}$ at $h = 50.0 \text{ cm Hg}$ and $E = -1.50 \text{ V}$ in ammoniacal buffer.

Electrochemical Measurements:

As the base solutions, $0.02 \text{ mol dm}^{-3} \text{ NaH}_2\text{PO}_4\text{-Na}_2\text{HPO}_4$ (pH 7.0), $0.1 \text{ mol dm}^{-3} \text{ tris-HCl}$ (pH 7.5 - 8.9), and $0.2 \text{ mol dm}^{-3} \text{ NH}_3\text{-NH}_4\text{Cl}$ (pH 9.0 - 10.2), containing $2 \times 10^{-4} \text{ mol dm}^{-3} \text{ Co(NH}_3)_6\text{Cl}_3$ were used. The ionic strength of the base solutions was adjusted to 0.2 mol dm^{-3} with KCl. Protein concentrations were determined spectrophotometrically using values of $E_{1\text{cm}}^{1\%}$ (276 nm) = 8.29 at pH 7.0 for SSI⁶⁵ (M.W. of dimer = 22,800), $E_{1\text{cm}}^{1\%}$ (279 nm) = 8.7 at pH 7.5 for PS⁶¹ (M.W. of dimer = 22,800), and $E_{1\text{cm}}^{1\%}$ (278nm) = 10.63 at pH 7.0 for S.BPN^{65,66} (M.W. = 27,500). All measurements were made under nitrogen atmosphere at $25.0 \pm 0.5 \text{ }^\circ\text{C}$ in a thermostat. Other details of the electrochemical measurements are described in previous chapters.

RESULTS AND DISCUSSION

SUBTILISIN BPN' - *STREPTOMYCES* SUBTILISIN INHIBITOR INTERACTION

Brdicka Current of SSI:

SSI gave well-defined Brdicka waves in d.c. polarography at mercury electrode in buffers of pH 7.0 to 10.0 (see Fig.6-1). Analysis of the polarograms has revealed that the catalytic currents, i_B , at -1.35 to -1.50 V are explained by Eq.(1-4) at the concentration of hexaaminecobalt (III) chloride, Co(III) , lower than $2 \times 10^{-4} \text{ mol dm}^{-3}$. At -1.35 to -1.50 V Γ is controlled solely by diffusion and given by Koryta equation (eq.(1-10)), at the protein concentration less than $2 \times 10^{-7} \text{ mol dm}^{-3}$ and $\tau = 4.07 \text{ s}$, in ammoniacal buffer of pH 9.5. At dme f_{Co} is given by Ilkovic equation (Eq.1-6)). Accordingly k_B values of SSI dimer can be calculated from Eq.(1-4); the results are given in Table 6-1. In this

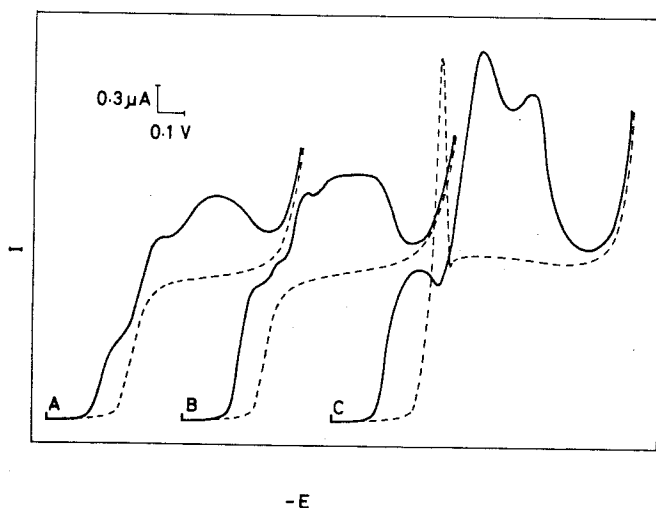


Fig.6-1. D.c. polarograms of $1.7 \times 10^{-7} \text{ mol dm}^{-3}$ SSI in the base solution of pH (A) 7.5, (B) 8.5, and (C) 9.5. Each curve starts from -0.8 V. The drop time was not regulated. Broken lines represent d.c. polarograms in the absence of SSI.

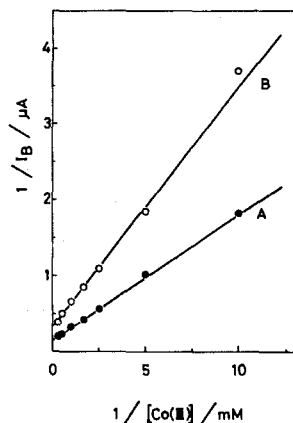


Fig.6-2. Dependence of $1/i_B$ on the concentration of Co(III) for the Brdicka currents of (A) $6.2 \times 10^{-8} \text{ mol dm}^{-3} (\text{SSI})_2$, and (B) (A) + $1.23 \times 10^{-7} \text{ mol dm}^{-3} \text{ S.BPN}'$ in the base solution of pH 9.5.

Table, N_S is the number of cysteine residues per one SSI dimer. Note that SSI exists as a dimer, $(\text{SSI})_2$, in the test solution.^{62,67)}

As described in chapter 1, the Brdicka current is expressed as a function of f_{Co} over a wide range of concentration of cobalt ion by Eq.(1-2) or (1-7). Fig.6-2 (plot A) shows that the Brdicka current of SSI is expressed by Eq.(1-7); from the plot, the values of $n_c k_c$ and k_f/k_d of SSI were estimated. The results are given in Table 6-1.

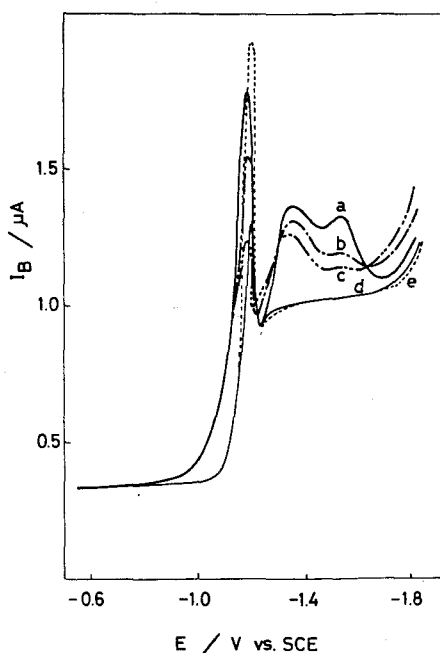


Fig.6-3. D.c. polarograms of (a) $4.7 \times 10^{-8} \text{ mol dm}^{-3} (\text{SSI})_2$, (b) (a) + $6.1 \times 10^{-8} \text{ mol dm}^{-3} \text{ S.BPN}'$, (c) (a) + $1.13 \times 10^{-8} \text{ mol dm}^{-3} \text{ S.BPN}'$, and (d) $6.4 \times 10^{-8} \text{ mol dm}^{-3} \text{ S.BPN}'$ in the base solution of pH 9.5. Curve e (dotted line) represents d.c. polarogram in the absence of protein.

Table 6-1. Brdicka Current Constants of SSI and S.BPN'-SSI Complex at -1.4 V in Ammoniacal Buffer of pH 9.5 (at 25 °C)

Protein	M.W. dalton	$\overset{a)}{D}_p$ $10^{-7} \frac{cm^2}{s}$	N_s	k_f/k_d $10^9 \frac{cm^2}{mol s}$	$\frac{n}{c} \frac{k_c}{c}$ $10^4 s^{-1}$	k_B $10^{13} \frac{cm^2}{mol s}$
SSI	11500 x 2	9.02	4 x 2	0.9	1.7	1.5
S.BPN'-SSI	39000 x 2	6.30	4 x 2	1.1	1.0	1.1

a) Calculated according to Svedberg equation, using reported values of sedimentation coefficient and partial specific volume.^{62,67)}

Direct Polarographic Titration of SSI with S.BPN' (or vice versa):

S.BPN', which contains neither cysteine nor cystine residues, did not give Brdicka wave (see curve d in Fig.6-3), but when S.BPN' was added to an SSI solution, the Brdicka current of SSI was reduced with addition of S.BPN', as shown in Fig.6-3, until a constant Brdicka wave was produced in the presence of a large excess of S.BPN' (curve c in Fig.6-3). On the contrary no change of the Brdicka waves of SSI was obtained when bovine milk α_{s1} -caseine (M.W. = 23,500), an independent protein containing neither SH- nor SS-group,⁶⁸⁾ was added up to about $1.7 \times 10^{-7} \text{ mol dm}^{-3}$ to a $2.4 \times 10^{-8} \text{ mol dm}^{-3}$ SSI solution. Accordingly, the decreasing of the Brdicka current heights of SSI with addition of S.BPN' must be attributed to the formation of complex of SSI with S.BPN', which is actually a dimeric complex, (S.BPN')(SSI)₂(S.BPN'), according to Inouye *et al.*,⁶⁷⁾

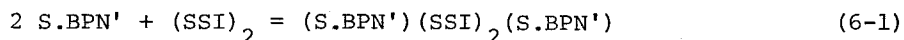


Fig.6-4 shows the Brdicka current heights at -1.40 and -1.50 V plotted against added amounts of S.BPN', indicating that SSI can be titrated amperometrically with S.BPN'. Conversely, S.BPN' can be titrated with SSI. The equivalent point of the complex formation was determined as $[S.BPN']:[(SSI)_2] = 2:1.01$ (titration at -1.40 V) or $2:1.04$ (titration at -1.50 V) in an ammoniacal buffer of pH 9.5 (Fig.6-4) and $2:1.02$ in a phosphate buffer of pH 7.0. D.c. polarographic method could also be applied to direct titration of $2.4 \times 10^{-8} \text{ mol dm}^{-3}$ of $(SSI)_2$ with S.BPN'. SSI can similarly be titrated with S.BPN' by potential sweep voltammetry based on the Brdicka current at hmde at the concentration level as low as $2.2 \times 10^{-9} \text{ mol dm}^{-3}$ of $(SSI)_2$ (see Fig.6-5).

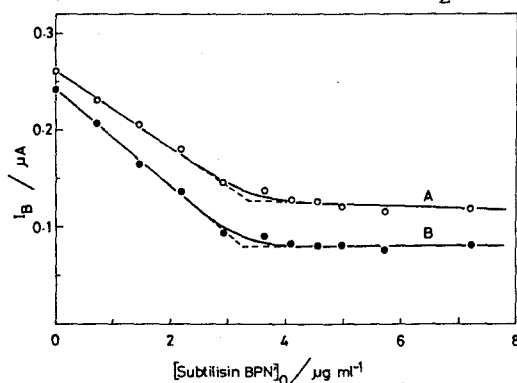


Fig.6-4. Dependence of the Brdicka current heights at (A) -1.40 V and (B) -1.50 V of $4.74 \times 10^{-8} \text{ mol dm}^{-3} (SSI)_2$ on addition amount of S.BPN' in the base solution of pH 9.5.

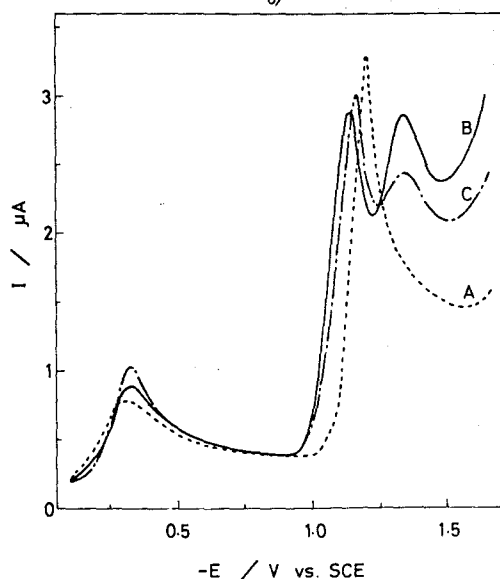


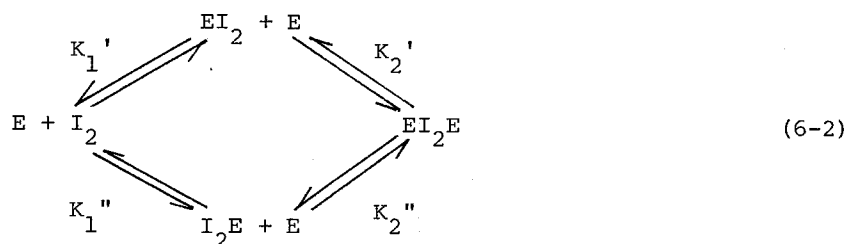
Fig.6-5. Voltage sweep voltammograms of (A) the base solution of pH 9.5, (B) (A) + $2.30 \times 10^{-9} \text{ mol dm}^{-3} (SSI)_2$, and (C) (B) + $6.0 \times 10^{-9} \text{ mol dm}^{-3} S.BPN'$. The hmde was exposed to the test solution for 2 min under stirring and for 1 min at stationary state, then the voltammograms were recorded at $v = -0.2 \text{ V s}^{-1}$.

Brdicka Current of (S.BPN')(SSI)₂(S.BPN') Complex:

The Brdicka current of SSI in the presence of a large excess of S.BPN', which is assigned to the S.BPN'-SSI complex as discussed above, was analyzed by Eqs.(1-2) to (1-11) to give the values of k_B , $n_C k_C$ and k_f/k_d of the complex (see plot B in Fig.6-2). The $n_C k_C$ value of S.BPN'-SSI complex is about one half the value of SSI, whereas the k_f/k_d values of S.BPN'-SSI complex and SSI are nearly of the same magnitude. Since it is reasonable to presume that k_C value of S.BPN'-SSI complex is of the same magnitude as that of SSI, these results can be interpreted as that the n_C value of S.BPN' value of S.BPN'-SSI complex is one half the value of SSI; that is one of two SS bonds of SSI monomer may become hardly accessible to Brdicka reaction by the complex formation. This interpretation is in harmony with a proposed structure of the S.BPN'-SSI complex based on x-ray crystallography⁶⁹; one SS bond (Cys(71)-Cys(101)) of SSI is in close vicinity of the reactive site of SSI (Met(73)-Val(74))⁷⁰ by which S.BPN' is strongly bound to form the S.BPN'-SSI complex, so that it may become hardly accessible to the Brdicka reaction, whereas another SS bond (Cys(35)-Cys(50)) of SSI is located far from the reactive site and may remain to be accessible to the Brdicka reaction.

Theory on Multiple Equilibrium of Dimeric Enzyme-Inhibitor Complex Dissociation:

When a bifunctional dimeric inhibitor, I_2 , binds successively two molecules of the enzyme, E, to form enzyme-inhibitor complexes. The complex formation is described by the following scheme,



In this scheme, K_1' , K_1'' , K_2' , and K_2'' are the elemental dissociation constants⁷¹⁾ (or microconstants of dissociation⁷²⁾), which involve the microscopically distinct forms;

$$\begin{aligned} K_1' &= \frac{[E][I_2]}{[EI_2]}, & K_2' &= \frac{[E][EI_2]}{[EI_2E]} \\ K_1'' &= \frac{[E][I_2]}{[I_2E]}, & K_2'' &= \frac{[E][I_2E]}{[EI_2E]} \end{aligned} \quad (6-3)$$

Also the overall dissociation constants⁷¹⁾ (or macroconstants of dissociation⁷²⁾) K_1 and K_2 are defined by

$$\begin{aligned} K_1 &= \frac{[E][I_2]}{([EI_2] + [I_2E])} = \frac{K_1'K_1''}{K_1' + K_1''} \\ K_2 &= \frac{[E]([EI_2] + [I_2E])}{[EI_2E]} = K_2' + K_2'' \end{aligned} \quad (6-4)$$

where $[E]$, $[I_2]$, $[EI_2]$, $[I_2E]$, and $[EI_2E]$ stand for the concentrations of free E, free I_2 , EI_2 , I_2E , and EI_2E , respectively. In our case two microscopic forms EI_2 and I_2E are physically indistinguishable, therefore we have

$$\begin{aligned} K_1' &= K_1'' = 2K_1 \\ K_2' &= K_2'' = K_2/2 \end{aligned} \quad (6-5)$$

We also have

$$[E]_0 = [E] + [EI_2] + [I_2E] + 2[EI_2E] \quad (6-6)$$

$$[I_2]_0 = [I_2] + [EI_2] + [I_2E] + [EI_2E] \quad (6-7)$$

where $[E]_0$ and $[I_2]_0$ are the analytical concentrations of E and I_2 . The Brdicka current intensity is proportional to the concentration of protein, as described in chapter 1. Therefore the total Brdicka current intensity, i_t , observed during the course of the titration of I_2 with E or *vice versa*, can be expressed as

$$i_t = \kappa_E [E] + \kappa_{I_2} [I_2] + \kappa_{EI_2} ([EI_2] + [I_2E]) + \kappa_{EI_2E} [EI_2E] \quad (6-8)$$

where κ_E , κ_{I_2} , κ_{EI_2} and κ_{EI_2E} are the proportional constants converting the protein concentrations to the Brdicka current intensities for E, I_2 , EI_2 (or I_2E) and EI_2E , respectively. The κ_p is characteristic of the protein P for a given electrode system.

We define Δi , the change in the Brdicka current intensity due to the complex formation, by

$$\Delta i = \kappa_E [E]_0 + \kappa_{I_2} [I_2]_0 - i_t \quad (6-9)$$

Upon substituting Eqs.(6-6) to (6-8) into Eq.(6-9) and assuming that

$$\kappa_{EI_2} = (\kappa_{I_2} + \kappa_{EI_2E})/2 \quad (6-10)$$

we get

$$\begin{aligned} \Delta i &= (1/2) (2\kappa_E + \kappa_{I_2} - \kappa_{EI_2E}) ([EI_2] + [I_2E] + 2[EI_2E]) \\ &= (1/2) (2\kappa_E + \kappa_{I_2} - \kappa_{EI_2E}) ([E]_0 - [E]) \end{aligned} \quad (6-11)$$

Also, Δi may be expressed by a relative change in Brdicka current, ΔI , defined by

$$\Delta I = \Delta i / (\kappa_{I_2} [E]_0 / 2)$$

$$= \Delta\kappa([E]_0 - [E])/[E]_0 \quad (6-12)$$

where

$$\Delta\kappa = (2\kappa_E + \kappa_{I_2} - \kappa_{EI_2E})/\kappa_{I_2} \quad (6-13)$$

On the other hand, $[E]$ is the solution of Eq.(6-14), which is derived from Eqs.(6-3) to (6-7),

$$[E]^3 + (2[I_2]_0 - [E]_0 + 2\kappa_2') [E]^2 + \kappa_2' (2[I_2]_0 - 2[E]_0 + \kappa_1') [E] - \kappa_1' \kappa_2' [E]_0 = 0 \quad (6-14)$$

Differential Pulse Polarographic Determination of Dissociation Constants of S.BPN'-SSI Complex:

The author has applied to the determination of dissociation constants of S.BPN'-SSI complex differential pulse (DP) polarographic method, which is more sensitive by about two orders of magnitude than d.c. polarography, as shown in chapter 5. In DP polarography, SSI gave a well defined Brdicka current polarogram or protein wave having two peaks (Fig.6-6, curve b). The height of the protein wave at the potential of the first peak, $E_{\max} = -1.28$ V at pH 10.0, increased linearly with increasing concentration of SSI solution. When S.BPN' was added to an SSI solution, the protein wave decreased in height as shown, for example, by curved d in Fig.6-6. The decrease in the current height of SSI with addition of S.BPN' should be attributed to the complex formation of SSI with S.BPN'. S.BPN' also gave a DP polarographic protein wave, though its peak height was very much smaller than that of SSI (Fig.6-6, curve c). Fig.6-7 shows a Δi vs. potential curve obtained at $[E]_0 = 9.4 \times 10^{-8}$ mol dm⁻³ and $[I_2]_0 = 4.7 \times 10^{-8}$ mol dm⁻³.

S.BPN' contains neither cysteine nor cystine residue⁶⁶⁾ and gave no Brdicka current in d.c. polarography. Accordingly, S.BPN' was expected to give no protein wave also in DP polarography. Thus, the

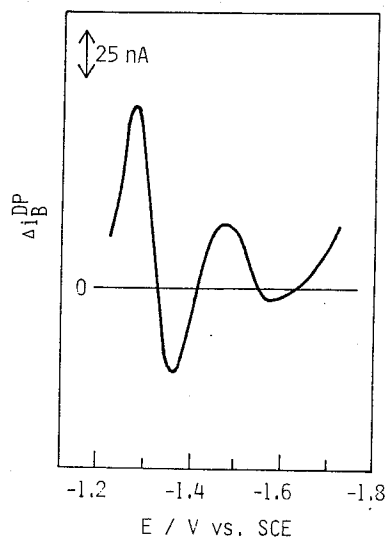
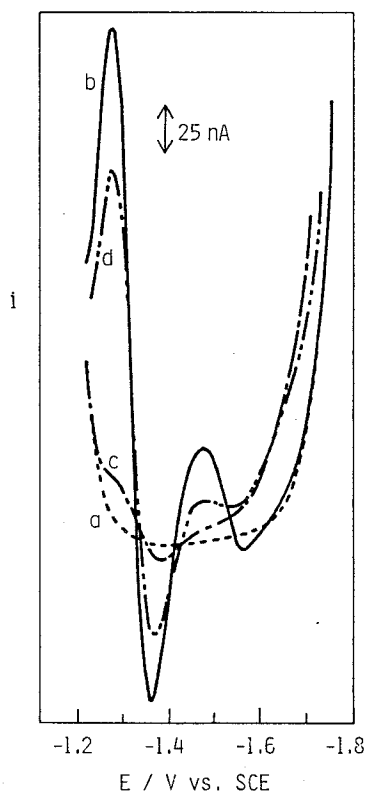


Fig.6-6 (left) Differential pulse polarograms of (a): the base solution of pH 10.0, (b): (a) + $4.7 \times 10^{-8} \text{ mol dm}^{-3}$ SSI, (c): (a) + $9.4 \times 10^{-8} \text{ mol dm}^{-3}$ S.BPN' and (d): (a) + $4.7 \times 10^{-8} \text{ mol dm}^{-3}$ SSI and $9.4 \times 10^{-8} \text{ mol dm}^{-3}$ S.BPN'. Polarograms were run from $E_i = -1.23 \text{ V}$ at $v = 1 \text{ mV s}^{-1}$, $\Delta E = -50 \text{ mV}$, and $\tau = 1.67 \text{ s}$.

Fig.6-7 (right) Δi_{DP} vs. potential curve for the complex formation between $9.4 \times 10^{-8} \text{ mol dm}^{-3}$ S.BPN' and $4.7 \times 10^{-8} \text{ mol dm}^{-3}$ SSI.

small DP polarographic wave observed with S.BPN' may most probably be attributed to trace impurities in the S.BPN' preparation. α -Amylase (*Bacillus subtilis*), which contains neither SH nor SS group,⁵⁶⁾ gave no DP polarographic protein wave. Following discussion on the dissociation constants is not affected, whether the small DP polarographic wave is due to the impurities in the S.BPN' preparation ($\kappa_E = 0$), or the enzyme

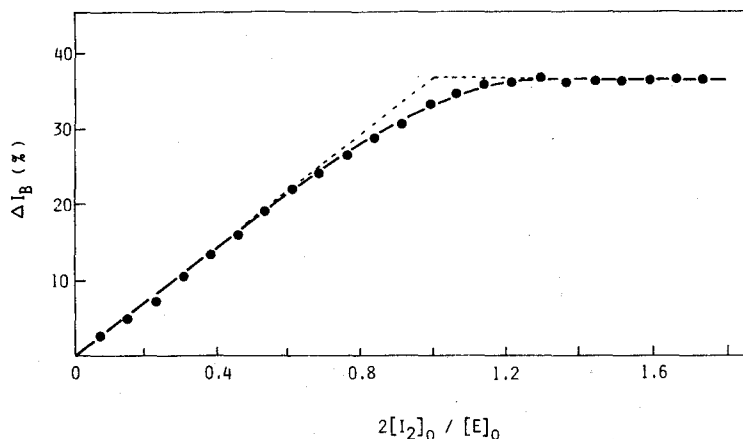


Fig.6-8. Polarographic titration curve (ΔI vs. $2[I_2]_0/[E]_0$ plot) of S.BPN' with SSI at the S.BPN' analytical concentration of $9.64 \times 10^{-9} \text{ mol dm}^{-3}$. The current was measured at $E_{\text{max}} = -1.28 \text{ V}$.

itself (κ_E is small).

Titration of $9.4 \times 10^{-8} \text{ mol dm}^{-3}$ S.BPN' with SSI was performed amperometrically at $E_{\text{max}} = -1.28 \text{ V}$, $\tau = 1.67 \text{ s}$, and $\text{pH} = 10.0$. Fig.6-8 shows the plot of ΔI against the added amount of SSI or $2[I_2]_0/[E]_0$ at $[E]_0 = 9.4 \times 10^{-8} \text{ mol dm}^{-3}$. The ΔI values initially increase linearly with $2[I_2]_0/[E]_0$ and reach a certain maximum value, $\Delta I_{\text{max}} = 0.37$, with an inflection point at $2[I_2]_0/[E]_0 = 1.0$, indicating that the complex formation between SSI and S.BPN' proceeds according to Eq.(6-1) and that the dissociation constants are so small that the concentrations of $(\text{S.BPN}')(\text{SSI})_2$ or $(\text{SSI})_2(\text{S.BPN}')$ (as well as free $(\text{SSI})_2$ at $2[I_2]_0/[E]_0 < 1$) is negligibly small compared with that of free S.BPN' plus $(\text{S.BPN}')(\text{SSI})_2(\text{S.BPN}')$ at such a relatively high concentration of S.BPN'. After ΔI reaches ΔI_{max} , that is at $2[I_2]_0/[E]_0 > 1$, free S.BPN' is vanishingly small. Then, $\Delta I_{\text{max}} = \Delta \kappa = 0.37$ since $[E]_0 \gg [E]$, which implies that $\kappa_{EI_2E} \approx 0.6\kappa_{I_2}$ since κ_E is zero or very small. These results can also be interpreted as one of two SS bonds of SSI monomer becomes inaccessible to Brdicka reaction by the complex formation.

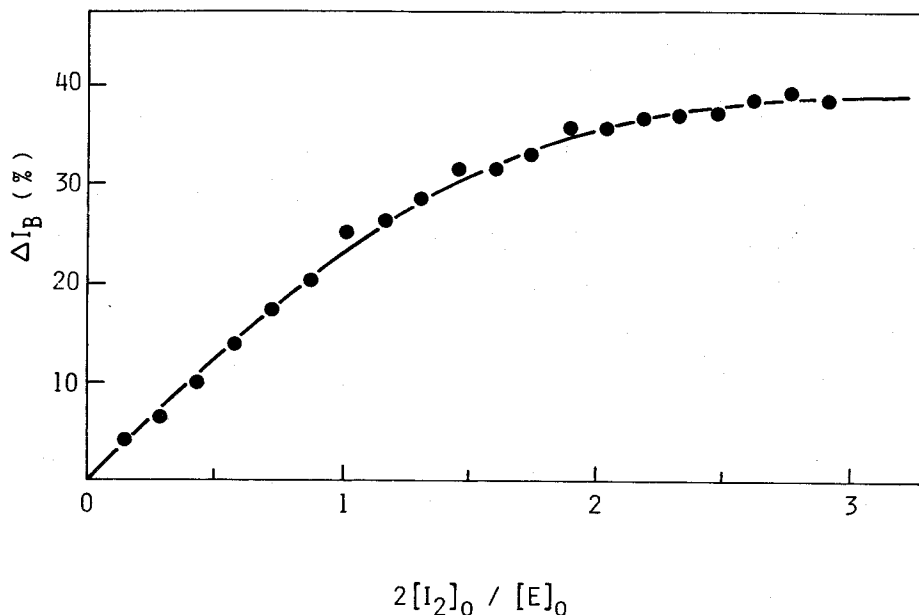


Fig.6-9. Polarographic titration curve (ΔI vs. $2[I_2]_0/[E]_0$ plot) of S.BPN' with SSI at the S.BPN' analytical concentration of $9.64 \times 10^{-9} \text{ mol dm}^{-3}$. The solid line is a regression curve calculated on values of $K_1' = 0.5 \times 10^{-9} \text{ mol dm}^{-3}$, $K_2' = 9.4 \times 10^{-9} \text{ mol dm}^{-3}$ and $\Delta\kappa = 0.40$.

Titration of S.BPN' with SSI was carried out also at $[E]_0 = 9.64 \times 10^{-9} \text{ mol dm}^{-3}$, as shown in Fig.6-9. The titration curve changes smoothly near the equivalent point ($2[I_2]_0/[E]_0 = 1$), indicating that the dissociation of S.BPN'-SSI complex should not be negligible at such a low concentration of S.BPN'. Thus we tried to fit to the ΔI vs. $2[I_2]_0/[E]_0$ plot the curve represented by Eqs.(6-12) and (6-14) by adjusting three parameters K_1' , K_2' and $\Delta\kappa$ (three-parameter model) using a Facom M-200 computer in Data Processing Center of Kyoto University. The results of the least-squares analysis using SALS program²⁸⁾ were $K_1' = (0.5 \pm 0.4) \times 10^{-9} \text{ mol dm}^{-3}$, $K_2' = (9.4 \pm 2.2) \times 10^{-9} \text{ mol dm}^{-3}$ and $\Delta\kappa = 0.40 \pm 0.02$ at pH=10.0, $I = 0.2 \text{ mol dm}^{-3}$, and $t = 25^\circ\text{C}$. Solid line in Fig.6-9 is a regression curve calculated on values of $K_1' = 0.5 \times 10^{-9} \text{ mol dm}^{-3}$, $K_2' = 9.4 \times 10^{-9} \text{ mol dm}^{-3}$ and $\Delta\kappa = 0.40$.

This $\Delta\kappa$ value agrees well with $\Delta I_{\max} = \Delta\kappa = 0.37$ estimated from the titration curve at $[E]_0 = 9.4 \cdot 10^{-8} \text{ mol dm}^{-3}$ (Fig.6-8).

We also tried to fit to the ΔI vs. $2[I_2]_0/[E]_0$ plot in Fig.6-9 the theoretical curve derived on assuming that all four elemental dissociation constants are equal; $K' = K_1' = K_1'' = K_2' = K_2''$, by adjusting two parameters, K' and $\Delta\kappa$ (two-parameter model). The results were $K' = (6.9 \pm 1.1) \times 10^{-9} \text{ mol dm}^{-3}$ and $\Delta\kappa = 0.54 \pm 0.02$. For purpose of statistical model identification, a minimum Akaike's information criterion (AIC) estimate⁷³⁾ was employed. According to Akaike,⁷³⁾ AIC is defined by $AIC = N \ln S + 2M$, where N , M and S are the number of data, the number of parameters and the residual sum of squares, respectively, and when there are several competing models, the fitting model which gives the minimum of AIC is a statistically maximum likelihood one. In our case, the AIC value of the three-parameter model was 52.3, whereas it was 68.7 for the two-parameter model. The former is appreciably smaller than the latter. Also, the $\Delta\kappa$ value for two-parameter model deviates appreciably from $\Delta I_{\max} = 0.37$. These results indicate that the three-parameter model is statistically better one than two-parameter model; in other words, K_1' differs from K_2' significantly. The ratio $K_1'/K_2' = 0.053$ implies that the intrinsic free energy change of the first binding of the enzyme to the inhibitor is $1.7 \text{ kcal mol}^{-1}$ larger than that of the second binding.

In conclusion, the above results show that the polarographic method based on Brdicka current can be applied for direct determination of the enzyme-inhibitor complex dissociation constants as low as $10^{-10} \text{ mol dm}^{-3}$. So far as the author knows, this is the first report describing that the intrinsic free energy change in the first binding of S.BPN' to dimeric SSI differs significantly from that of the second binding.

SUBTILISIN BPN' - PLASMINOSTREPTIN INTERACTION

Brdicka Currents of PS and S.BPN'-PS Complex:

PS is a protein proteinase inhibitor containing two SS bonds per monomer, of which the amino acid sequence is identical with that of SSI at about 70 % of the positions,⁷⁴⁾ and gave well defined Brdicka waves at mercury electrode in buffers of pH 7.5 to 10.2 (see Fig.6-10). The d.c. or fast polarographic Brdicka current at -1.35 V increased linearly with increasing concentration of the protein, up to $8.0 \times 10^{-7} \text{ mol dm}^{-3}$ in a tris buffer of pH 8.5 with dme of $\tau = 1.52 \text{ s}$. When S.BPN' was added to a PS solution, the Brdicka current of PS decreased with addition of S.BPN' and *vice versa*, as shown in Fig.6-11. The Broken line in this Figure shows Δi (defined by Eq.(6-9)) *vs.* potential curve, obtained at $[E]_0 = 2.0 \times 10^{-7} \text{ mol dm}^{-3}$ and $[I_2]_0 = 1.0 \times 10^{-7} \text{ mol dm}^{-3}$ in fast polarographic mode.

Titration of $2.86 \times 10^{-7} \text{ mol dm}^{-3}$ S.BPN' with PS was performed amperometrically at $E_m = -1.35 \text{ V}$, $\tau = 1.25 \text{ s}$ by fast polarography.

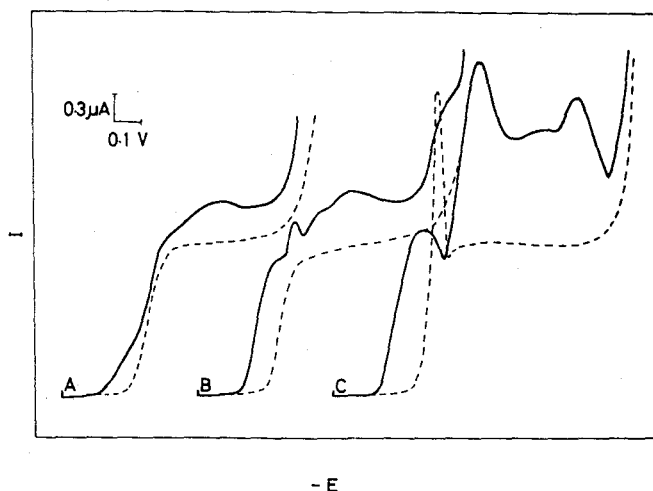


Fig.6-10. D.c. polarograms of $1.75 \times 10^{-7} \text{ mol dm}^{-3} (\text{PS})_2$ in the base solution of pH (A) 7.5, (B) 8.5 and (C) 9.5. Each curve starts from -0.8 V. The drop time was not regulated. Broken lines represent d.c. polarograms in the absence of PS.

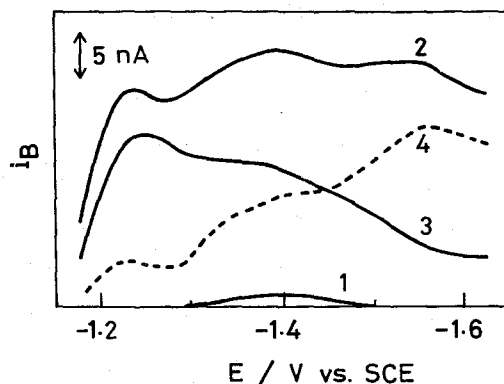


Fig.6-11. Fast polarographic protein wave of (1) $2.0 \times 10^{-7} \text{ mol dm}^{-3}$ S.BPN', (2) $1.0 \times 10^{-7} \text{ mol dm}^{-3}$ $(\text{PS})_2$ and (3) $2.0 \times 10^{-7} \text{ mol dm}^{-3}$ S.BPN' and $1.0 \times 10^{-7} \text{ mol dm}^{-3}$ $(\text{PS})_2$ in the base solution of pH 8.0.

The current was measured from the limiting current of the base solution. Dotted line (curve 4) represents Δi vs. potential curve for the complex formation between $2.0 \times 10^{-7} \text{ mol dm}^{-3}$ S.BPN' and $1.0 \times 10^{-7} \text{ mol dm}^{-3}$ $(\text{PS})_2$.

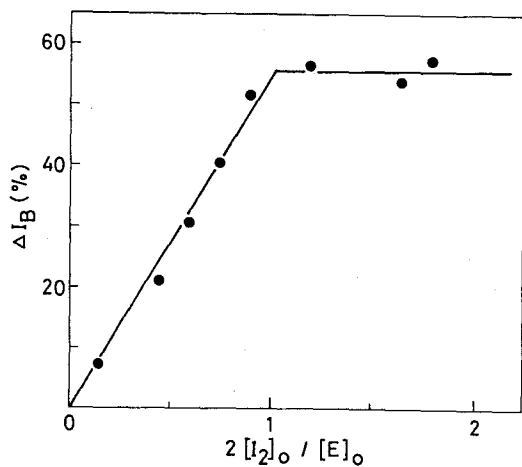


Fig.6-12. Fast polarographic titration curve (ΔI vs. $2[I_2]_0/[E]_0$ plot) of S.BPN' with PS at the S.BPN' analytical concentration of $2.86 \times 10^{-7} \text{ mol dm}^{-3}$. The current was measured at $E_m = -1.35 \text{ V}$.

Fig.6-12 shows the plot of ΔI (defined by Eq.(6-12)) against the amount of PS or $2[I_2]_0/[E]_0$ at pH 8.5. The ΔI values initially increase linearly with $2[I_2]_0/[E]_0$ and reach a certain maximum value, $\Delta I_{\max} = 0.55$, with an inflection point at $2[I_2]_0/[E]_0 = 1.0$, indicating that PS binds one molecule of S.BPN' per one subunit of PS to form S.BPN'-PS complex. The value of $\Delta I_{\max} = \Delta\kappa = 0.55$ can be interpreted as one of two SS bonds in PS monomer, which may be Cys(67)-Cys(97) in close vicinity of the reactive site of PS (Lys(67)-Gly(70)),⁷⁴ may become inaccessible to Brdicka reaction by the complex formation.

Determination of Dissociation Constants of S.BPN'-PS Complex:

Titration of S.BPN' with PS was carried out also at $[E]_0 = 4.56 \times 10^{-8} \text{ mol dm}^{-3}$ and pH = 8.5 as shown in Fig.6-13. PS exists as a dimer in tris buffer of pH 7.5.⁶¹ Upon assuming that S.BPN'-PS complex is dimeric, $(\text{S.BPN}')(\text{PS})_2(\text{S.BPN}')$, the author determined the dissociation constants of S.BPN'-PS complex by the same way as in the case of S.BPN'-SSI complex. The results were $K_1' = (6.7 \pm 4.8) \times 10^{-9} \text{ mol dm}^{-3}$, $K_2' = (1.2 \pm 0.7) \times 10^{-8} \text{ mol dm}^{-3}$, and $\Delta\kappa = 0.55 \pm 0.01$. The solid line in Fig.6-13 is a regression curve calculated on values of $K_1' = 6.7 \times 10^{-9} \text{ mol dm}^{-3}$ and $K_2' = 1.2 \times 10^{-10} \text{ mol dm}^{-3}$ and $\Delta\kappa = 0.55$, according to Eqs.(6-12) and (6-14). This $\Delta\kappa$ value also agree well with $\Delta I_{\max} = \Delta\kappa = 0.55$ estimated from the titration curve at $[E]_0 = 2.86 \times 10^{-7} \text{ mol dm}^{-3}$ (Fig.6-12).

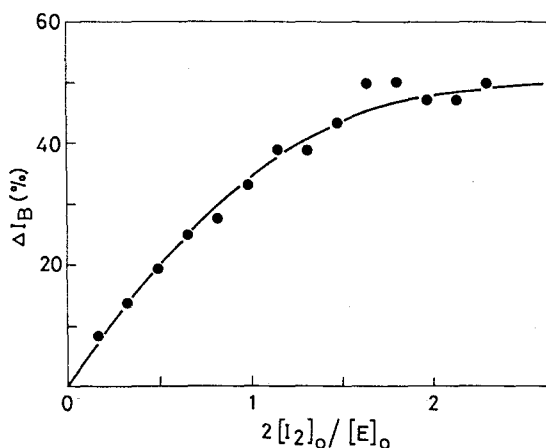


Fig.6-13. Fast polarographic titration curve (ΔI vs. $2[I_2]_0/[E]_0$ plot) of S.BPN' with PS at the S.BPN' analytical concentration of $4.56 \times 10^{-8} \text{ mol dm}^{-3}$. The solid line is a regression curve calculated on values of $K_1' = 6.7 \times 10^{-9} \text{ mol dm}^{-3}$, $K_2' = 1.2 \times 10^{-10} \text{ mol dm}^{-3}$ and $\Delta\kappa = 0.55$.

As in the case of S.BPN'-SSI complex. The ratio $K_1'/K_2' = 0.56$ implies that the intrinsic free energy of the first binding of the enzyme to the inhibitor is $0.34 \text{ kcal mol}^{-1}$ larger than that of the second binding.

Effect of pH on Dissociation Constants of S.BPN'-PS Complex:

The author also determined the intrinsic dissociation constants of S.BPN'-PS complex at pH 7.8 to 10.2. Fig.6-14 shows the pH dependence of the intrinsic dissociation constants or pK' ($= -\log K'$) vs. pH plots (Dixon plots⁷⁵) of the first and second binding of S.BPN' to PS. The broken lines in Fig.6-14 are so-called guide lines of Dixon plots, whose slopes are zero and -1, and show

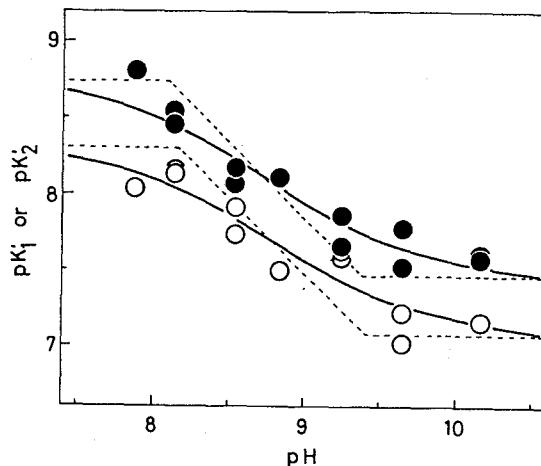
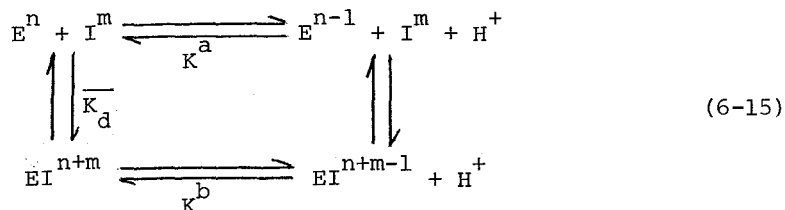


Fig.6-14. Effect of pH on K_1' (●) and on K_2' (○) of S.BPN'-PS complexes. Dotted lined represent guide lines.

suggest that one ionizable group in the reactant protein species and another ionizable group in the product protein species participate in the first and/or second binding of S.BPN' with PS.

Here we consider simple bimolecular interaction system between enzyme and inhibitor, where enzyme and complex exist in two states of ionization, as follows;



In this scheme, superscripts represent the number of ionizable protons in protein species and we will assume that the form of E^n of the enzyme combines with inhibitor I^m with pH-independent dissociation constant, $\overline{K_d}$, defined by

$$\overline{K_d} = \frac{[E^n][I^m]}{[EI^{n+m}]} \quad (6-16)$$

K^a and K^b refer to the ionization state of the enzyme and the enzyme-inhibitor complex, respectively, that is

$$K^a = \frac{[E^n][H^+]}{[E^n]} \quad (6-17)$$

$$K^b = \frac{[EI^{n+m-1}][H^+]}{[EI^{n+m}]} \quad (6-18)$$

We use for convenient the subscript t to denote the sum of the concentrations of all different forms of the enzyme and the complex; thus for this system we have

$$[E]_t = [E^n] + [E^{n-1}] \quad (6-19)$$

$$[EI]_t = [EI^{n+m}] + [EI^{n+m-1}] \quad (6-20)$$

Apparent dissociation constant K_d can be expressed by

$$K_d = \frac{[E]_t [I^n]}{[EI]_t} \quad (6-21)$$

Upon substituting Eqs.(6-16) to (6-20) into Eq.(6-21), we can get

$$pK_d = p\overline{K_d} + \log(1 + 10^{pH-pK^b}) - \log(1 + 10^{pH-pK^a}) \quad (6-22)$$

Eq.(6-22) can be applied to the system where inhibitor exists in two states of ionization, $I^m \rightleftharpoons I^{m-1} + H^+$, instead of E. Then K^a and K^b can generally be considered to refer to the ionization state of the reactant (the enzyme or the inhibitor in this scheme) and the product (the enzyme-inhibitor complex), respectively. Also above discussion is available for the microscopic dissociation equilibrium of E and I_2 . Thus, we get, for the first stage of microscopic dissociation of EI_2 (or I_2E),

$$pK_1' = \overline{pK_1'} + \log(1 + 10^{pH-pK_1^b}) - \log(1 + 10^{pH-pK_1^a}) \quad (6-23)$$

and for the second stage of microscopic dissociation of EI_2E ,

$$pK_2' = \overline{pK_2'} + \log(1 + 10^{pH-pK_2^b}) - \log(1 + 10^{pH-pK_2^a}) \quad (6-24)$$

We tried to fit the curve represented by Eqs.(6-23) and (6-24) to the pK_1' and pK_2' vs. pH plots, by adjusting three parameters $\overline{K_1'}$, K_1^a , and K_1^b , and $\overline{K_2'}$, K_2^a and K_2^b , respectively. The results of the least-squares analysis using SALS program²⁸⁾ were $\overline{pK_1'} = 8.74 \pm 0.17$, $pK_1^a = 8.10 \pm 0.23$ and $pK_1^b = 9.38 \pm 0.22$ for the first binding step, and $\overline{pK_2'} = 8.31 \pm 0.17$, $pK_2^a = 8.17 \pm 0.28$ and $pK_2^b = 9.40 \pm 0.26$ for the second binding step. The difference in $\overline{pK_1'}$, $\overline{pK_1'} - \overline{pK_2'} = 0.43$, implies that the pH-independent intrinsic free energy change of the first binding of the enzyme to the inhibitor is $0.6 \text{ kcal mol}^{-1}$ larger than that of the second binding. The pK_1^a value and pK_1^b value do not significantly differ from pK_2^a and pK_2^b , respectively, and pK_1^a or pK_2^a is smaller by about one unit than pK_1^b or pK_2^b .

The pK_1^a or pK_2^a value obtained here ($8.1 \sim 8.2$) is slightly higher than those so far reported $pK = 5 \sim 6$, if it is assumed to represent the pK of histidine at the active site of S.BPN' (serine-enzyme),⁷⁶⁾ as suggested by Uehara *et al.*,⁶³⁾ who reported the involvement of an ionizable group of pK 8.5 in the association of S.BPN' and SSI. A contribution of ionizable group of lysin in PS or tyrosine in S.BPN' may not be excluded.

Although whether these ionizable groups of pK_1^a , pK_2^a , pK_1^b , and pK_2^b exist in S.BPN' or PS is not clear, these results may be interpreted as that pK value of a ionizable group of S.BPN' or PS in the free state ($pK = 8.1 \sim 8.2$) increases by about one unit ($pK = 9.4$) due to the complex formation between S.BPN' and PS.

The determination of the dissociation constant of the S.BPN'-PS complex described above is based on the assumption of dimeric S.BPN'-PS complex formation. Then, the results may be considered as tentative, since according to Kakinuma *et al.*⁶¹⁾ trypsin-PS complex exists in a monomeric form in tris buffer of pH 7.5. Further study is continued.

SUMMARY

Brdicka currents of SSI and PS have been studied by d.c., tast, and differential pulse polarographic techniques and potential sweep voltammetric technique. The Brdicka current of SSI or PS decreased with addition of S.BPN', which was attributed to the formation of proteinase-inhibitor complexes. Analysis of the dependences of Brdicka currents of SSI and S.BPN'-SSI complex on cobalt ion concentration revealed that one of two SS bonds of SSI became hardly accessible to Brdicka reaction by the complex formation. SSI and PS could be directly titrated by polarographic technique based on the Brdicka current in the concentration level of 10^{-7} to 10^{-9} mol dm⁻³.

The first and second dissociation constants of S.BPN'-SSI and S.BPN'-PS complexes as low as 10^{-8} to 10^{-10} mol dm⁻³ were determined by fitting to the titration data theoretical curves, in which the multiple equilibrium involving microscopically distinct forms of S.BPN'-inhibitor complex was taken into account. The intrinsic free energy change in the first binding of S.BPN' to dimeric SSI or PS was larger than that of the second binding.

The effect of pH on the intrinsic dissociation constants of S.BPN'-PS complex has suggested the participation of ionizable groups with

$pK = 8.1$ and 9.4 in the first step and of ionizable groups with $pK = 8.2$ and 9.4 in the second step of binding.

Chapter 7. POLAROGRAPHIC STUDY ON INTERACTION BETWEEN HUMAN IgG AND SHEEP ANTI-HUMAN IgG ANTISERUM AND ITS ANALYTICAL APPLICATION^{j)}

Immunoglobulin is a protein containing disulfide bonds and hence produces Brdicka current. In this chapter the author has applied d.c. and differential pulse polarographic techniques for the study of the complex formation of human immunoglobulin G (IgG) with sheep antihuman IgG antiserum (anti-IgG) at the concentration level as low as 10^{-10} mol dm⁻³. The (average) intrinsic dissociation constant of the IgG - anti-IgG complex has been determined. The results also suggest a possible analytical application of Brdicka current coupled with the immunochemical reaction.

EXPERIMENTAL

Materials:

Lyophilized preparation of human immunoglobulin G (IgG) was a gift of Wako Pure Chemical Industries, Ltd. and used as received. The concentration of IgG was determined spectrophotometrically using $E_{1\text{cm}}^{1\%}(280\text{ nm}) = 15.0$.⁷⁷⁾ Affinity chromatographic liquid preparation of sheep antihuman IgG antiserum (anti-IgG) was also a gift of Wako Pure Chemical Industries, Ltd. and used as received. The titer of the anti-IgG preparation was 2.0 mg antibody per cm³, as determined by the quantitative precipitation reaction. The molecular weights of IgG and anti-IgG were estimated at 160,000.⁷⁸⁾ The optimum proportion of anti-IgG to IgG in the precipitation reaction was 5:1. All other chemicals were of reagent grade quality.

Apparatus:

D.c. polarograms were recorded with a Yanagimoto polarograph P-8,

equipped with a Yanagimoto drop controller P-8-RT, and differential pulse polarograms were recorded with a Yanagimoto voltammetric analyzer P-1000, equipped with a Watanabe recorder WX-4401. The characteristics of the dropping mercury electrode were $m = 0.852 \text{ mg s}^{-1}$ and $\tau = 11.08 \text{ s}$ at $h = 50.0 \text{ cm Hg}$ and $E = -1.50 \text{ V}$ in an ammoniacal buffer. In recording polarograms the drop time was controlled at $\tau = 2.0 \text{ s}$, unless otherwise stated.

Electrochemical Measurements:

As the base solution, $0.1 \text{ mol dm}^{-3} \text{ NH}_3 - 0.1 \text{ mol dm}^{-3} \text{ NH}_4\text{Cl} - 0.1 \text{ mol dm}^{-3} \text{ KCl}$ buffer solution (pH 9.5 and the ionic strength $I = 0.2 \text{ mol dm}^{-3}$) containing $2 \times 10^{-4} \text{ mol dm}^{-3} \text{ Co}(\text{NH}_3)_6\text{Cl}_3$ was used. All measurements were made under nitrogen atmosphere at $25.0 \pm 0.5^\circ \text{C}$ in a thermostat. Other details of the electrochemical measurements have been described in previous chapters.

RESULTS AND DISCUSSION

D.c. Polarograms of IgG, anti-IgG and their Mixture:

In d.c. polarography, IgG and anti-IgG gave a well-defined protein wave due to Brdicka current, as shown by polarograms (1) and (2), respectively, in Fig.7-1. The Brdicka current, i_B , usually measured at -1.35 V from the limiting current of cobalt ion, increased linearly with the concentration of IgG or anti-IgG up to about $6 \times 10^{-8} \text{ mol dm}^{-3}$. As described in chapter 6, Brdicka current is additive of each contribution. Actually, when a small amount of bovine pancreas ribonuclease-A (RNase), as indifferent protein to anti-IgG, was added to $2.5 \times 10^{-8} \text{ mol dm}^{-3}$ anti-IgG in the base solution, the Brdicka current increased additively with addition of RNase up to $2.2 \times 10^{-7} \text{ mol dm}^{-3}$. On the contrary, when IgG was added to $2.5 \times 10^{-8} \text{ mol dm}^{-3}$ anti-IgG in the base solution, the Brdicka current did not additively increase but the Brdicka current of

the mixture of IgG and anti-IgG was always smaller than the sum of the Brdicka currents of IgG and anti-IgG (see Fig.1, curve 3). This result may be explained by that with addition of IgG to an anti-IgG solution IgG - anti-IgG complexes are formed and that the SS bonds in the proteins become inaccessible to Brdicka reaction by the complex formation, as described in chapter 6.

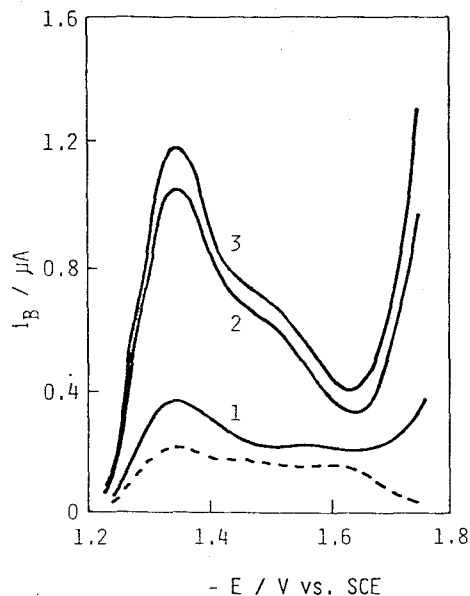


Fig.7-1. D.c. polarographic Brdicka currents of 1) $2.44 \times 10^{-8} \text{ mol dm}^{-3}$ IgG, 2) $2.50 \times 10^{-8} \text{ mol dm}^{-3}$ anti-IgG, and 3) $2.44 \times 10^{-8} \text{ mol dm}^{-3}$ IgG + $2.50 \times 10^{-8} \text{ mol dm}^{-3}$ anti-IgG in the base solution. The Brdicka current, i_B , was measured from the limiting reduction current of cobalt ion. Broken line represents Δi_B vs. potential curve (see text). $h = 60.7 \text{ cm Hg}$, $\tau = 2.0 \text{ s}$.

In Fig.7-1, curves 1, 2 and 3 represent d.c. polarographic Brdicka currents produced by $2.44 \times 10^{-8} \text{ mol dm}^{-3}$ IgG, $2.50 \times 10^{-8} \text{ mol dm}^{-3}$ anti-IgG and $2.44 \times 10^{-8} \text{ mol dm}^{-3}$ IgG plus $2.50 \times 10^{-8} \text{ mol dm}^{-3}$ anti-IgG, respectively. We define *difference* Brdicka current, Δi_B , by

$$\Delta i_B = i_B([Ag]_0) + i_B([Ab]_0) - i_B([Ag]_0 + [Ab]_0) \quad (7-1)$$

where $i_B([Ag]_0)$, $i_B([Ab]_0)$ and $i_B([Ag]_0 + [Ab]_0)$ are the Brdicka currents produced by antigen (IgG in our case) at the concentration of $[Ag]_0$, antibody (anti-IgG) at the concentration of $[Ab]_0$, and their mixture at the concentrations of $[Ag]_0$ and $[Ab]_0$ in the base solution, respectively. Broken line in Fig.7-1 shows a Δi_B vs. potential curve at $[Ag]_0 = 2.44 \times 10^{-8} \text{ mol dm}^{-3}$ and $[Ab]_0 = 2.50 \times 10^{-8} \text{ mol dm}^{-3}$.

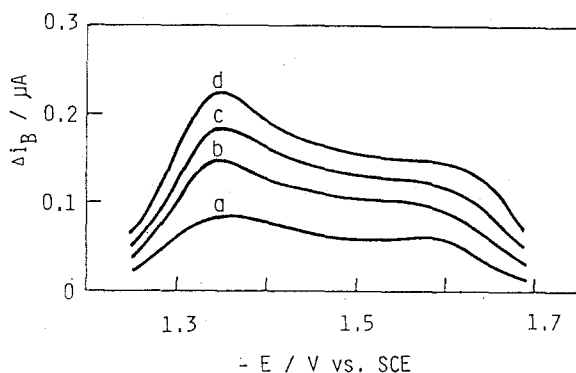


Fig.7-2. ΔI_B vs. potential curves observed with mixtures of IgG and anti-IgG at the concentrations of $2.50 \times 10^{-8} \text{ mol dm}^{-3}$ anti-IgG with a) $6.1 \times 10^{-8} \text{ mol dm}^{-3}$, b) $1.22 \times 10^{-8} \text{ mol dm}^{-3}$, c) $1.88 \times 10^{-8} \text{ mol dm}^{-3}$, and d) $2.44 \times 10^{-8} \text{ mol dm}^{-3}$ IgG.

As seen in Fig.7-2, the ΔI_B vs. potential curve has two humps at -1.35 V and -1.60 V, respectively. Subsequent addition of IgG results in incremental increase in the difference Brdicka current, as shown in Fig.7-2. Fig.7-3 shows three plots of the relative difference Brdicka currents, ΔI_B , defined by

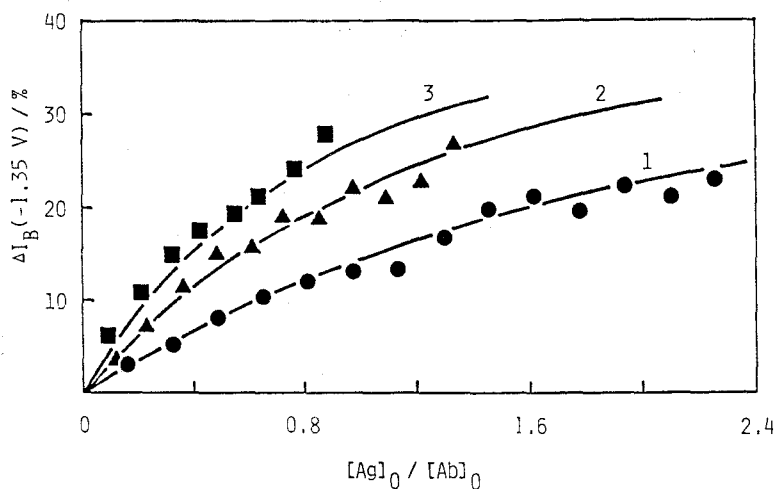


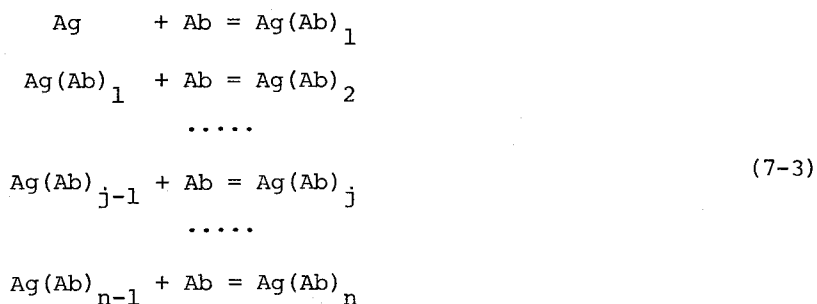
Fig.7-3. D.c. polarographic titration of anti-IgG with IgG (calibration curves for IgG) at the concentrations of a) $1.25 \times 10^{-8} \text{ mol dm}^{-3}$, b) $2.50 \times 10^{-8} \text{ mol dm}^{-3}$, and c) $3.75 \times 10^{-8} \text{ mol dm}^{-3}$. The solid lines are regression curves calculated on values of $K = 1.3 \times 10^{-7} \text{ mol dm}^{-3}$ and $\Delta K = 0.48$.

$$\Delta I_B = \Delta i_B / i_B ([Ab]_0) \quad (7-2)$$

against the added amount of IgG represented by $[Ag]_0/[Ab]_0$ at $[Ab]_0 = 1.25, 2.50, \text{ and } 3.75 \times 10^{-8} \text{ mol dm}^{-3}$. The ΔI_B value increases with $[Ag]_0/[Ab]_0$ and tends to approach a certain limiting value.

Determination of Dissociation Constants of IgG - anti-IgG Complexes:

Mathematical formulation of the antigen-antibody complex formation is very complicated, since generally both antigen and antibody are multivalent. In the following, we limit our discussion to the primary interaction of antigen and antibody and adopt following assumptions for simplification. We assume first that all the binding sites of the n-valent antigen are of equal affinity with the antibody and behave independently from each other. We also assume that the antibody behaves as monovalent ligand in the complex formation. Then the formation of the antigen (Ag) - antibody (Ab) complex is expressed by,



In these equations, the protein species represented by $Ag(Ab)_j$ involves ${}_nC_j$ species of microscopically distinct $Ag(Ab)_j$ complex. We also have

$$K = \frac{[Ag][Ab]}{[Ag(Ab)_1]} = \frac{[Ag(Ab)_{j-1}][Ab]}{[Ag(Ab)_j]} \quad (j = 2, 3, \dots, n) \quad (7-4)$$

where K is the (average) intrinsic dissociation constant of the binding

site of antigen with antibody, and $[Ag]$, $[Ab]$ and $[Ag(Ab)_j]$ are the concentrations of free antigen, free antibody and individual microscopic form of $Ag(Ab)_j$, respectively. We further have

$$[Ag]_0 = [Ag] + \sum_{j=1}^n n C_j [Ag(Ab)_j] \quad (7-5)$$

$$[Ab]_0 = [Ab] + \sum_{j=1}^n j C_j [Ag(Ab)_j] \quad (7-6)$$

The Brdicka current intensities, $i_B([Ag]_0)$, $i_B([Ab]_0)$ and $i_B([Ag]_0 + [Ab]_0)$ in Eq.(1) can be expressed by

$$i_B([Ag]_0) = \kappa_{Ag} [Ag]_0 \quad (7-7)$$

$$i_B([Ab]_0) = \kappa_{Ab} [Ab]_0 \quad (7-8)$$

$$i_B([Ag]_0 + [Ab]_0) = \kappa_{Ag} [Ag] + \kappa_{Ab} [Ab] + \sum_{j=1}^n \kappa_{Ag(Ab)_j} n C_j [Ag(Ab)_j] \quad (7-9)$$

where κ_{Ag} and κ_{Ab} are the proportional constants converting the concentrations of antigen and antibody to their Brdicka currents, respectively, and $\kappa_{Ag(Ab)_j}$ is the proportional constant for the microscopic forms of $Ag(Ab)_j$ assumed to have the same proportional constant for a given j . Note that κ_p 's are characteristic of the proteins, P , for a given polarographic technique with a given electrode system. It is reasonable to assume that $\kappa_{Ag(Ab)_j}$ changes with j in an arithmetical series,

$$\kappa_{Ag(Ab)_j} = j \kappa_{Ag(Ab)_1} - (j - 1) \kappa_{Ag} \quad (j = 1, 2, \dots, n) \quad (7-10)$$

Upon substituting Eqs.(5) to (10) into Eq.(1) we get

$$\begin{aligned}\Delta I_B &= (\kappa_{Ag} + \kappa_{Ab} - \kappa_{Ag(Ab)_1}) \sum_{j=1}^n J_n C_j [Ag(Ab)_j] \\ &= (\kappa_{Ag} + \kappa_{Ab} - \kappa_{Ag(Ab)_1}) ([Ab]_0 - [Ab])\end{aligned}\quad (7-11)$$

Also upon substituting Eqs.(4), (5), (6) and (11) into Eq.(2), we get

$$\Delta I_B = (\Delta\kappa/2[Ab]_0) (n[Ag]_0 + [Ab]_0 + K - \sqrt{(n[Ag]_0 - [Ab]_0 + K)^2 + 4K[Ag]_0}) \quad (7-12)$$

where

$$\Delta\kappa = (\kappa_{Ag} + \kappa_{Ab} - \kappa_{Ag(Ab)_1})/\kappa_{Ab} \quad (7-13)$$

We fitted the curve represented by Eq.(12) with $n = 5$ (see EXPERIMENTAL) to the ΔI_B vs. $[Ag]_0/[Ab]_0$ plots in Fig.7-3 by adjusting two parameters K and $\Delta\kappa$ using a Facom M-200 computer in Data Processing Center of Kyoto University. The results of the least-squares analysis are $K = (1.3 \pm 1.0) \times 10^{-7} \text{ mol dm}^{-3}$ and $\Delta\kappa = 0.48 \pm 0.20$ at pH 9.5, $I = 0.2 \text{ mol dm}^{-3}$ and 25°C . Solid lines in Fig.7-3 are regression curves calculated on values of $K = 1.3 \times 10^{-7} \text{ mol dm}^{-3}$ and $\Delta\kappa = 0.48$. This K value $1.3 \times 10^{-7} \text{ mol dm}^{-3}$ seems a reasonable one,⁷⁹⁾ though this value should be considered in views of the assumptions adopted for simplification as an average value representing the affinity of binding between IgG and anti-IgG.

Analytical Application:

The ΔI_B vs. $[Ag]_0/[Ab]_0$ curves in Fig.3 can be used as the calibration curves for the determination of IgG at the concentration level of $(2 \sim 40) \times 10^{-9} \text{ mol dm}^{-3}$.

Differential pulse (DP) polarographic technique is more sensitive than d.c. polarographic one to detect proteins using Brdicka current as described in chapter 5. Fig.7-4 shows DP polarographic Brdicka currents

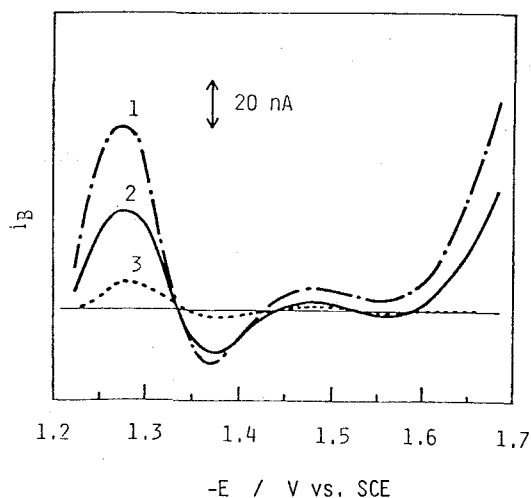


Fig.7-4. Differential pulse polarographic Brdicka currents of
 1) 5.5×10^{-9} mol dm $^{-3}$ IgG,
 2) 2.5×10^{-9} mol dm $^{-3}$ anti-IgG
 and 3) Δi_B vs. potential curve
 observed with a mixture of 5.5×10^{-9} mol dm $^{-3}$ IgG and 2.5×10^{-9} mol dm $^{-3}$ anti-IgG. $h = 56.0$ cm Hg, $\tau = 3.0$ s.

of IgG (curve 1) and anti-IgG (curve 2), and Δi_B vs. potential curve observed with a mixture of IgG and anti-IgG (curve 3). The Δi_B vs.

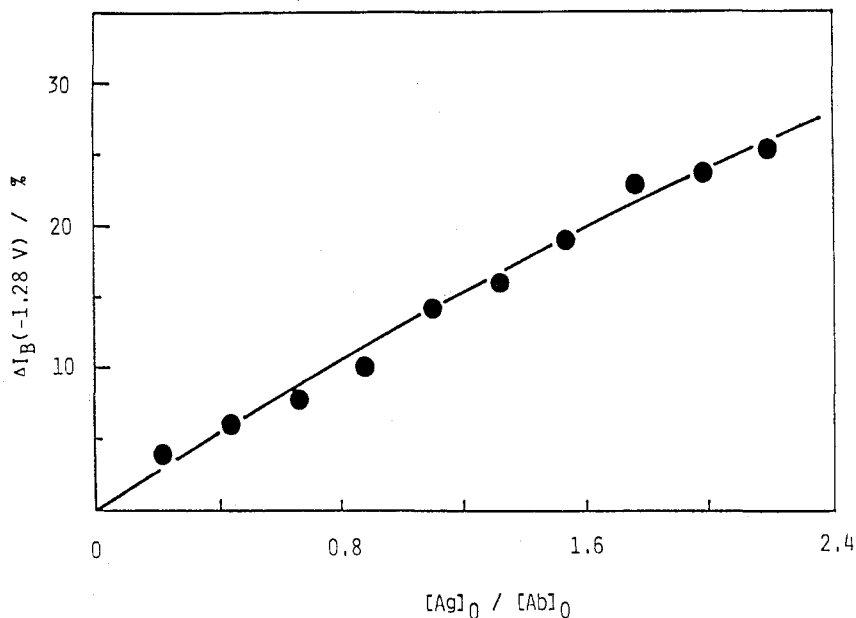


Fig.7-5. A calibration curve for $(5 \sim 5.5) \times 10^{-10}$ mol dm $^{-3}$ IgG obtained at the anti-IgG concentration of 2.5×10^{-9} mol dm $^{-3}$ by the differential pulse polarographic method.

potential curve in DP polarography has a peak at -1.28 V. Direct titration of anti-IgG with IgG was performed amperometrically at the fixed potential of -1.28 V. Fig.7-5 shows a ΔI_B vs. $[Ag]_0/[Ab]_0$ curve or a calibration curve at $[Ab]_0 = 2.5 \times 10^{-9} \text{ mol dm}^{-3}$. These results reveal that the DP polarographic method based on Brdicka current can be used for detection of IgG as low as $10^{-10} \text{ mol dm}^{-3}$.

Calibration curves for the determination of antibody, *i.e.* ΔI vs. $[Ag]_0/[Ab]_0$ plots, can similarly be constructed. Application of this method for detection of hapten may be possible by replacing antigen with hapten in the above calibration curves (Figs.7-3 and 7-5).

The present polarographic method of analysis based on Brdicka current coupled with antigen-antibody complex formation can be characterized by its considerably high sensitivity. Also this method does not require the labeling of the reagents (antibody or antigen) with radio active isotopes, enzyme or fluorescent molecules, as employed in conventional immunoassay techniques.⁸⁰⁾ Co-existing substances, so far as they are Brdicka-inactive, do not interfere with the determination. However, the co-existence of proteins which are indifferent to the interest immunoreaction but Brdicka-active, if present in a large excess, should interfere with the determination.

SUMMARY

Brdicka currents of human immunoglobulin G (IgG) and sheep antihuman IgG antiserum (anti-IgG) were studied by d.c. and differential pulse polarographic techniques. The Brdicka current of a mixture of IgG and anti-IgG was smaller than the sum of the currents of IgG and anti-IgG. This difference in current is attributed to the primary complex formation between IgG and anti-IgG. Anti-IgG could be directly titrated with IgG (or *vice versa*) by the polarographic technique based on the difference in Brdicka current. The average intrinsic dissociation constant was

estimated from the titration curve. The polarographic method based on Brdicka current coupled with the immunoreaction can be used to determine trace amounts of antigen (or antibody) as low as 10^{-10} mol dm⁻³ using the differential pulse polarographic technique.

CONCLUSION

In this study, the polarographic catalytic hydrogen current or Brdicka current of proteins was investigated with intent to light on fundamentals and applications of Brdicka current.

In PART I, the author has studied fundamental of Brdicka current. First, basic equation of Brdicka current is presented, in which Brdicka current is expressed by a function of the surface concentration of protein, the bulk concentration of cobalt ion and two parameters, $n_c k_c$ and k_f/k_d , where n_c is the number of the total sites, on which the complex can be formed, in a protein molecule, and k_c and k_f/k_d are the (average) constants representing the intrinsic catalytic activity and the life time, respectively, of the complex. The theoretical equation has been experimentally verified with respect to the dependence of Brdicka current on the conditions of electrode system as well as the concentrations of protein, cobalt salts. The method to determine the two parameters $n_c k_c$ and k_f/k_d has been established.

Brdicka current activities $k_B = n_c k_c (k_f/k_d)$ or $n_c k_c$ and k_f/k_d of SS (or SH) group, heme c group and S-(ethylsuccinimide)group were determined. The difference in their activities between these three groups has been found as mainly due to the difference in the stability (k_f/k_d).

Effects of ammonia buffer concentration, C_{amm} , pH and temperature on $n_c k_c$ and k_f/k_d values have been investigated. The dependence of $n_c k_c$ on C_{amm} indicated that water molecule as well as ammonium ion participates in the catalytic reaction as a proton donor. The k_f/k_d value slightly decreases with C_{amm} , suggesting participation of ammonia molecule in the protein-Co(0) complex formation. The sigmoidal pH-dependence has been found for $n_c k_c$ and k_f/k_d values corrected for the effect of buffer salts. This has been interpreted as due to the ionization of functional group (probably sulfhydryl group) in adsorbed protein. With increasing temperature, the $n_c k_c$ value increases, but k_f/k_d value decreases. The decrement of k_f/k_d is larger than the increment of $n_c k_c$, resulting in the decrease in overall catalytic activity with temperature.

The apparent activation energy of the electrochemical hydrogen evolution reaction has been established.

On the basis of the basic equation of Brdicka current, theoretical expressions of normal pulse (NP) and differential pulse (DP) polarographic Brdicka currents have been derived. These equations well explain the experimental results of NP and DP polarographic Brdicka current.

Pulse polarographic study on Brdicka current has revealed that at the less negative potential than -1.40 V the protein SSI (*Streptomyces subtilisin inhibitor*) is adsorbed strongly and irreversibly on mercury electrode and the surface concentration is controlled solely by diffusion. At more negative potential than -1.50 V the adsorption of SSI becomes weak with increasing negative potential and the surface concentration is controlled by both diffusion and adsorption. The latter is dependent on the electrode potential.

In PART II, the author has studied applications of Brdicka current. First, DP polarographic technique based on Brdicka current has been developed. Amperometry has been performed by applying a fixed potential of E_{\max} (= -1.28 V), which corresponds with the potential of the first maximum of the DP polarographic Brdicka current of the protein. The Brdicka current at E_{\max} is linearly depends on the protein concentration in the range between $3 \mu\text{g cm}^{-3}$ and 5 ng cm^{-3} . Amperometry under non-deaerated conditions has also been studied, in which protein as low as 20 ng cm^{-3} can be detected.

Second, Brdicka currents of SSI and PS (plasminostreptin) have been studied by d.c., tast, and DP polarographic techniques and potential sweep voltammetric technique. The Brdicka current of SSI or PS decreased with addition of subtilisin BPN' (S.BPN'), which is attributed to the formation of proteinase-inhibitor complexes. Analysis of the dependence of Brdicka currents of SSI and S.BPN'-SSI complex on cobalt ion concentration revealed that one of two SS bonds of SSI became hardly accessible to Brdicka reaction by the complex formation. SSI and PS could be directly titrated by polarographic technique based on Brdicka current in the concentration level of 10^{-7} to $10^{-9} \text{ mol dm}^{-3}$.

The first and second dissociation constants of S.BPN'-SSI and S.BPN'-PS complexes as low as 10^{-8} to 10^{-10} mol dm⁻³ were determined by fitting to the titration data theoretical curves, in which the multiple equilibrium involving microscopically distinct forms of S.BPN'-inhibitor complex was taken into account. The intrinsic free energy change in the first binding of S.BPN' to dimeric SSI or PS was larger than that of the second binding.

The effect of pH on the intrinsic dissociation constants of S.BPN'-PS complex has suggested the participation of ionizable groups with pK = 8.1 and 9.4 in the first step and of ionizable groups with pK = 8.2 and 9.4 in the second step of binding.

In the last chapter, Brdicka currents of human immunoglobulin G (IgG) and sheep antihuman IgG antiserum (anti-IgG) were studied by d.c. and DP polarographic techniques. The Brdicka current of a mixture of IgG and anti-IgG was smaller than the sum of the currents of IgG and anti-IgG. This difference in current is attributed to the primary complex formation between IgG and anti-IgG. Anti-IgG could be directly titrated with IgG (or *vice versa*) by the polarographic technique based on the difference in Brdicka current. The average intrinsic dissociation constant was estimated from the titration curve. The polarographic method based on Brdicka current coupled with the immunoreaction can be used to determine trace amounts of antigen (or antibody) as low as 10^{-10} mol dm⁻³ using the DP polarographic technique.

ACKNOWLEDGEMENTS

The author wishes to express his deep gratitude to Dr. Mitsugi Senda, Professor of Kyoto University. His scientific insight, patience and personal concern have been invaluable contributions to this research. The author is also grateful to Dr. Tokuji Ikeda, Associate Professor of Kyoto University for his continuous guidance and valuable advice in carrying out this work.

It is a great pleasure to acknowledge the interest and discussion on S.BPN'-SSI interaction of Dr. Keitaro Hiromi, Professor of Kyoto University and Dr. Ben'ichiro Tonomura, Associate Professor of Kyoto University, and the encouragement of Dr. Tanekazu Kubota, Professor of Gifu College of Pharmacy.

The author is grateful to Dr. Sawao Murao, Professor of Osaka Prefecture University and Dr. Keitaro Hiromi for their kind gift of SSI preparation, to Dr. Atsushi Kakinuma, Takeda Chemical Industries, Ltd., for his kind gift of PS preparation, and to Osaka Research Laboratory of Wako Pure Chemical Industries, Ltd. for the kind gift of IgG and anti-IgG preparations.

Thanks are due to Mr. Ichiro Tokimitsu and Miss Sachiko Ibe for their many helpful collaborations. The kind suggestions and the continuous encouragements by Dr. Tadaaki Kakutani, Dr. Takashi Kakiuchi, Dr. Hiromichi Morikawa and Dr. Junko Takeda, instructors of Kyoto University, and Dr. Hideaki Kinoshita, Professor of Kwassui Women's College, during this work are gratefully acknowledged.

The author is indebted to members of the Laboratory of Chemistry and Physics of Biopolymer, Department of Agricultural Chemistry, Kyoto University for their helpful suggestions and discussion.

REFERENCES

- 1) J.Heyrovsky and J.Babicka, Collect. Czech. Chem. Commun., 2, 370 (1930).
- 2) S.G.Mairanovskii, "Catalytic and Kinetic Waves in Polarography", trans. by B.M.Fabuss and P.Zuman, Plenum Press, N.Y., 1968, p.269.
- 3) R.Brdicka, Collect. Czech. Chem. Commun., 5, 112,148 (1933).
- 4) T.Ikeda, H.Kinoshita, Y.Yamane and M.Senda, Bull. Chem. Soc. Jpn., 53, 112 (1980).
- 5) H.Kinoshita, T.Ikeda, Y.Yamane and M.Senda, Agric. Biol. Chem., 44, 2337 (1980).
- 6) T.Ikeda, H.Kinoshita, T.Konishi and M.Senda, Paper presented at the 26th Annual Meeting of Polarography in Fukuoka, Oct. 14-15th, 1980; Abstract, Rev. Polarogr. (Kyoto), 26, 61 (1980).
- 7) J.Homolka, "Methods of Biochemical Analysis", Vol.19, ed. by D.Glick 1971, p.435.
- 8) M.Senda, "Rinshokensa-Zensho", Vol.5, ed. by Y.Matsumura, Igakushoin, 1977, p.331.
- 9) H.Berg, "Topics in Bioelectrochemistry and Bioenergetics", Vol.1, ed. by G.Millazo, John Wiley & Sons, London, New York, Sydney, Tronto, 1976, p.39.
- 10) M.Senda and T.Ikeda, Bunseki, 1977, 780.
- 11) M.Senda and T.Ikeda, Bunseki, 1982, 577.
- 12) M.Senda, T.Ikeda and H.Kinoshita, Bioelectrochem. Bioenerg., 3, 253 (1976).
- 13) I.M.Kolthoff, K.Yamashita and Tan Boen Hie, J. Electroanal. Chem., 63, 393 (1975).
- 14) G.Munshi and V.Kalous, Collect. Czech. Chem. Commun., 42, 1929 (1976).
- 15) G.Ruttekay-Nedecky, B.Bezuch and V.Vesela, Bioelectrochem. Bioenerg., 4, 399 (1977).
- 16) H.Kinoshita, Ph.D. Thesis, Kyoto University, 1979.
- 17) I.M.Kolthoff and P.Mader, Anal. Chem., 42, 1762 (1970).
- 18) B.A.Kuznetsov, Experientia Suppl., 18, 381 (1971).

- 19) I.M.Kolthoff, K.Yamashita, Tan Boen Hie and A.Kanbe, Proc. Nat. Acad. Sci. U.S.A., 70, 2020 (1973).
- 20) T.Ikeda, H.Kinoshita, Y.Yamane, K.Kano, Y.Ichikawa and M.Senda, Paper presented at the 24th Annual Meeting of Polarography in Sendai, Sep. 29-20th, 1978; Abstract, Rev. Polarogr. (Kyoto), 24, 63 (1980).
- 21) A.A.Vlcek, Z.Electrochem., 61, 1014 (1957).
- 22) J.Koryta, Collect. Czech. Chem. Commun., 18, 206 (1953).
- 23) D.G.Smith, O.O.Blumenfeld and W.Konigsberg, Biochem. J., 91, 589 (1964).
- 24) R.Jaenike, D.Schmid and S.Knof, Biochemistry, 7, 919 (1968).
- 25) W.D.Butt and D.Keillin, Proc. Roy. Soc. London, Ser. B, 156, 429 (1962).
- 26) E.Scheller, M.Janchen and H-J.Prumke, Biopolymer, 14, 1553 (1975).
- 27) J.Klumpar, Collect. Czech. Chem. Commun., 13, 11 (1948).
- 28) T.Nakagawa and Y.Oyanagi, "SALS User's Manual", Computer Center of Tokyo University, 1979.
- 29) K.Kutova, M.Brezina, Collect. Czech. Chem. Commun., 31, 743 (1966).
- 30) Y.Weber, J.Koutecky and J.Koryta, Z. Electrochem., 63, 583 (1959).
- 31) I.M.Kolthoff, H.Sawamoto and S.Kihara, J. Electroanal. Chem., 88, 233 (1978).
- 32) J.Kadlecek, P.Anzenbacher and V.Kalous, J. Electroanal. Chem., 86, 417 (1978).
- 33) J.Zikan and V.Kalous, Collect. Czech. Chem. Commun., 31, 4513 (1966).
- 34) H.Sunahara, D.N.Ward and A.C.Griffin, J. Am. Chem. Soc., 82, 6017 (1960).
- 35) G.Charlot, "Teisei-bunseki Kagaku", Vol.2, trans. by K.Sone and M.Tanaka, Kyoritsu Schuppan, 1958, p.290.
- 36) O.H.Muller, "Methods of Biochemical Analysis", Vol.11, ed. by D.Glick, 1963, p.329.
- 37) J.Heyrovsky and J.Kuta, "Principles of Polarography", Academic Press, New York (1966).
- 38) B.Alexandrov, M.Brezina and V.Kalous, Collect. Czech. Chem. Commun., 28, 210 (1963).
- 39) T.Ikeda, Y.Yamane, H.Kinoshita and M.Senda, Bull. Chem. Soc. Jpn., 53, 686 (1980).
- 40) I.Tokimitsu, M. Sc. Thesis, Kyoto University, 1982.

- 41) M.Brezina and V.Gultjaj, Collect. Czech. Chem. Commun., 28, 181 (1963).
- 42) A.L.Lehninger, "Biochemistry" 2nd ed., Worth Publishers, Inc., 1975, p.71.
- 43) I.M.Kolthoff and S.Kihara, Collect. Czech. Chem. Commun., 45, 669 (1980).
- 44) I.Watanabe and T.Shimanouchi, "Seibutsu Butsuri Kagaku Jikkenhoh", Baifukan, 1962, p.9.
- 45) I.M.Kolthoff, K.Yamashita, Tan Boen Hie and A.Kanbe, J. Electroanal. Chem., 53, 417 (1974).
- 46) R.G.Bates, "Electrometric pH Determination", John Wiley and Sons, Inc., New York, 1954, p.108.
- 47) G.C.Barker, Z. Anal. Chem., 173, 79 (1960).
- 48) J.Osteryoung and E.Kirowa-Eisner, Anal. Chem., 52, 62 (1980).
- 49) M.T.Stankovich and A.J.Bard, J. Electroanal. Chem., 86, 189 (1978).
- 50) T.Ikeda, K.Toriyama and M.Senda, Bull. Chem. Soc. Jpn., 52, 1937 (1979).
- 51) E.Palecek, V.Brabec and F.Jelen, J. Electroanal. Chem., 75, 471 (1977).
- 52) E.Palecek and Z.Pechan, Anal. Biochem., 42, 59 (1971).
- 53) M.Vorlickova and E.Palecek, Biochem. Biophys. Acta, 331, 276 (1973).
- 54) J.H.Crisie, J.Osteryoung and R.A.Osteryoung, Anal. Chem., 45, 210 (1973).
- 55) D.J.Myers and J.Osteryoung, Anal. Chem., 46, 356 (1974).
- 56) J.M.Junge, E.A.Stein, H.Neurath and E.H.Fisher, J. Biol. Chem., 234, 556 (1956).
- 57) J.L.Bailey, "Techniques in Protein Chemistry", Elsevier, Amsterdam, N.Y., 1967, p.340.
- 58) K.Sugawara and M.Fukushima, "Seibutsu-Jikkenhoh", Vol.7, ed. by I.Uritani, K.Shimura, M.Nakamura and M.Funatsu, Tokyo Daigaku Shuppankai, 1977, p.12.
- 59) P.W.Alexander and M.H.Shah, Talanta, 26, 97 (1979).
- 60) S.Murao and S.Sato, Agric. Biol. Chem., 36, 160 (1972).
- 61) A.Kakinuma, H.Sugino, N.Moriya and M.Isono, J. Biol. Chem., 253, 1529 (1978).
- 62) S.Sato and S.Murao, Agric. Biol. Chem., 38, 587, 2227 (1974).
- 63) Y.Uehara, B.Tonomura and K.Hiromi, J. Biochem., 84, 1195 (1978).
- 64) H.Sugino, N.Morira, S.Nakagawa, A.Kakinuma, M.Isono, S.Iwanaga,

- J.Takeda Research Lab., 37, 119 (1978).
- 65) K.Inouye, B.Tonomura, K.Hiromi, S.Sato and S.Murao, J.Biochem., 82, 961 (1977).
 - 66) F.S.Markland and E.L.Smith, J. Biol. Chem., 242, 5798 (1967).
 - 67) K.Inouye, B.Tonomura, K.Hiromi, T.Tanaka, H.Inagaki, S.Sato and S.Murao, J. Biochem., 84, 843 (1978).
 - 68) J.C.Mercier, F.Grosclaude and B. Ribadeau-Dumas, Eur. J. Biochem., 23, 41 (1971).
 - 69) Y.Mitsui, Y.Watanabe and S.Hirono, Tanpakushitsu Kakusan Koso, 24, 96 (1979).
 - 70) T.Ikenaka, S.Odani, M.Sakai, Y.Nabeshima, S.Sato and S.Murao, J. Biochem. 76, 1191 (1974).
 - 71) N.Bjerrum, Z. Physik. Chem., 106, 219 (1923).
 - 72) R.B.Martin, "Introduction to Biophysical Chemistry", McGraw-Hill, New York, San Francisco, Tronto, London, 1964, p.48.
 - 73) H.Akaike, IEEE Trans. Automat. Contr. AC-19, 667, 716 (1974).
 - 74) H.Sugino, A.Kakinuma and S.Iwanaga, J. Biol. Chem., 233, 1546 (1978).
 - 75) M.Dixon, E.C.Webb, C.J.R.Thorne and K.F.Tipton, "Enzymes", 3rd ed., Longman Group Ltd., 1979, p.138.
 - 76) W.R.Finkenstadt and M.Jr.Laskowski, "Proteinase Inhibitors", ed. by H.Fritz, H.Tscheshe, L.J.Greene and E.Truscheit, Springer-Verlag, Berline, 1974, p.389.
 - 77) J.Lisowski, M.Janusz, B.Tyran, A.Morawiecki, S.Golab and H.Bialkowska, Immunochemistry, 12, 159 (1975).
 - 78) R.R.Porter, Biochem. J., 46, 473 (1950).
 - 79) J.R.Sportsman and G.S.Wilson, Anal. Chem., 52, 2013 (1980).
 - 80) T.Matsushashi, H.Nariuchi, M.Usui, "Men'ekigaku-Nyumon", Gakkaishuppan Center, Tokyo, 1981, p.137.

- a) M.Senda, T.Ikeda, T.Kakutani, K.Kano and H.Kinoshita, Bioelectrochem. Bioenerg., 8, 151 (1981).
- b) M.Senda, T.Ikeda, K.Kano, and I.Tokimitsu, Bioelectrochem. Bioenerg., 9, 253 (1982).
- c) K.Kano, I.Tokimitsu, T.Ikeda and M.Senda, Paper presented at the 26th Annual Meeting of Polarography in Fukuoka, Oct. 14-15th, 1980; Abstract, Rev. Polarogr. (Kyoto), 26, 59 (1980).
- d) I.Tokimitsu, K.Kano, T.Ikeda and M.Senda, Paper Presented at the 26th Annual Meeting of Polarography in Fukuoka, Oct. 14-15th, 1980; Abstract, Rev. Polarogr. (Kyoto), 26, 60 (1980).
- e) I.Tokimitsu, K.Kano, T.Ikeda and M.Senda, Paper presented at the 27th Annual Meeting of Polarography in Yokohama, Oct. 17-18th, 1981; Abstract, Rev. Polarogr. (Kyoto), 27, 85 (1981).
- f) K.Kano, I.Tokimitsu, T.Ikeda and M.Senda, Paper presented at the 27th Annual Meeting of Polarography in Yokahama, Oct. 17-18th, 1981; Abstract, Rev. Polarogr. (Kyoto), 27, 84 (1981).
- g) K.Kano, T.Ikeda and M.Senda, Agric. Biol. Chem., 45, 233 (1981).
- h) K.Kano, T.Ikeda and M.Senda, Agric. Biol. Chem., in press.
- i) K.Kano, S.Ibe, T.Ikeda and M.Senda, to be submitted for publication.
- j) K.Kano, T.Ikeda and M.Senda, submitted to Agric. Biol. Chem.